CHAPTER 2

Transmitter Receptor Systems in Cingulate Regions and Areas

Nicola Palomero-Gallagher and Karl Zilles

Chapter contents

Transmitter receptors are heterogeneously distributed throughout the cerebral cortex and provide a novel and functionally relevant insight into the regional organization of the cortex, which cannot be achieved by architectonic observations in cell body- or myelin-stained sections alone. The regional distribution of transmitter receptors reflects well-established cyto- and myeloarchitectonically defined borders of cortical areas, and enables the additional identification of more cortical areas than previously demonstrated (Zilles and Palomero-Gallagher, 2001; Zilles *et al.*, 2003).

The mapping of different receptor binding sites is a novel and powerful tool which reveals the receptor-architectonic organization of the cerebral cortex (Zilles *et al.*, 1995, 2002a, 2002b; Morosan *et al.*, 2004). A single neuron expresses a variety of receptor subtypes of different neurotransmitter systems and, therefore, a single architectonical area will contain many different receptor subtypes. Furthermore, interactions between neurotransmitter systems are common (Atzori *et al.*, 2003; West *et al.*, 2003; Akiyama *et al.*, 2004; Drew and Vaughan, 2004; Lee *et al.*, 2004; Trudeau, 2004; Franco *et al.*, 2005), so that synaptic signalling mediated by a given neurotransmitter can be altered as a consequence of previous alterations in other neurotransmitter systems. Thus, it would be desirable to study as many different subtypes of receptors from as many different neurotransmitter systems as possible to obtain a comprehensive portrayal of such a complex system as that constituted by a cortical area.

We examined the laminar and regional distribution patterns of 15 different receptors for the classical neurotransmitters glutamate (AMPA, kainate, and NMDA receptors), GABA ($GABA_A$ and $GABA_B$ receptors, $GABA_A$ associated benzodiazepine binding sites), acetylcholine (muscarinic M_1, M_2 and M_3 as well as nicotinic receptors), noradrenaline (α_1 and α_2 receptors), serotonin ($5\text{-}HT_{1A}$ and $5\text{-}HT_2$ receptors), and dopamine (D_1 receptors) by means of quantitative *in vitro* receptor autoradiography. Additional neighbouring sections were stained for comparisons based on cyto- or myeloarchitectonic criteria. Since a single receptor does not necessarily reveal all borders, it can define a neurochemical family of cortical areas with a similar function. However, there is close agreement in the location of structural borders that are displayed by several receptors. These borders can coincide with cytoarchitectonical borders and they can also reveal the existence of hitherto unknown subdivisions.

Analysis of 15 transmitter receptors presents new statistical challenges as well as solutions to assessing the functional organization of cortical regions. Multivariate models have been applied to this data to parcellate parietal cortex and distinguish the medial, lateral, and cingulate sulcal divisions of area 5 (Scheperjans *et al.*, 2005). Although the cingulate area 5Ci can be detected with Nissl preparations and distinguished from areas 5M and 23c, this identification is quite subtle. The binding of NMDA, $GABA_B$, and α_1 receptors clearly show these borders in individual cases but the data are complex and difficult to relate. A hierarchical cluster analysis was used to integrate information from the multiple transmitter receptor systems and confirmed the presence of unique divisions of area 5 (Scheperjans *et al.*, 2005). Another strategy for assessing the relative densities of particular transmitters in an area and to compare and differentiate among many areas is the use of receptor fingerprints (Zilles *et al.*, 2002a). This tool displays binding sites in polar coordinate plots. The lines connecting the mean densities of the receptor types measured in each cytoarchitecturally identified cortical area define the contour of the fingerprint and the shapes and sizes of the fingerprints are specific for each area.

These powerful ligand binding methods have not been systematically applied to the human cingulate gyrus. In addition to establishing the transmitter features of each area and region, in the long term, these findings may help to identify pharmaceutical agents that will best target particular cingulate areas and regions for therapeutic intervention in the many cingulate-mediated diseases discussed throughout this volume.

Goals of this Chapter

This chapter presents an overview of the complex receptor balance present in the healthy human cingulate cortex. In order to do so, we shall:

- Provide a comprehensive description of the laminar and regional distribution patterns of 15 different receptors for classical neurotransmitters in the cingulate areas and regions of the parcellation scheme proposed by Vogt and collaborators (Vogt *et al.*, 1995, 2001; Vogt and Vogt, 2003; Vogt *et al.*, 2003).
- Describe the heterogeneities in receptor densities which enable the definition of new borders within areas 24c and 24c'. Each of these areas can be subdivided into a portion located on the ventral wall of the cingulate sulcus (24cv and 24c'v) and a portion restricted to the dorsal wall of the cingulate sulcus (24cd and 24c'd). Interestingly, area 24c, which is involved in emotion, contains the head area of the rostral cingulate motor area and projects to the facial motor nucleus. Thus, it is in excellent position to mediate the expression of facial emotion and its regulation by specific transmitter systems is of particular interest.
- Present the "receptor fingerprints" (Zilles *et al.*, 2002a) of the examined cingulate areas and discuss the

insights they provide into the four-region neurobiological model of the cingulate cortex based on the result of multivariate analysis procedures.

- Understand how the neurochemical structure of the *healthy* cingulate cortex may help target the mechanisms which underlie neuropathologic changes. Since specific brain regions are more vulnerable than others to certain diseases, not all neurotransmitter systems are necessarily involved in these changes. The selective vulnerabilities of cingulate subregions to particular diseases is a recurring theme throughout this volume and one important part of defining these and therapeutic targets is with ligand binding.

Cingulate-Section Autoradiography Method

Unfixed frozen slabs comprising the whole cross section of a human hemisphere were serially sectioned in the coronal plane. Figure 2.1 shows the medial surface from one case with the orientation of sections marked for each subsequent figure.

Alternating sections were processed for the visualization of different receptors for the neurotransmitters glutamate, GABA, acetylcholine, noradrenalin, serotonin, and dopamine as well as for histological stainings (silver cell body and myelin staining). The *in vitro* autoradiographical labeling method is carried out following standardized protocols (Zilles *et al.*, 2002a; Zilles *et al.*, 2002b). In short, it consists of three steps: a preincubation, a main incubation with the radiolabelled ligand and a rinsing step. Non-specific binding was determined in the presence of a respective unlabelled compound, which acted as a blocker. Radioactively labelled sections were then co-exposed with standards containing known concentrations of radioactivity against a tritium-sensitive film. After development of the film, the spatial distribution of optical densities in the ensuing autoradiographs, which were subsequently digitised and processed by densitometry with a video-based image analysing technique, indicates the local concentration of radioactivity present in the brain tissue, and thus represents a measure of the local binding site concentrations. For a detailed methodological review, see Zilles and collaborators (2002a, 2002b). Furthermore, autoradiographs were pseudo-colour coded to provide a clear visual impression of the regional and laminar distribution patterns of receptors. The gray values of each transformed autoradiograph were first linearly contrast enhanced, thus maintaining the absolute scaling between gray values and receptor densities while improving the visual presentation of the images. The full range of gray values obtained after contrast enhancement was then pseudo colour coded by assigning eleven colours in a spectral sequence to equally spaced gray value ranges.

Sections processed for histological staining served as a "template" to identify the cingulate regions and areas described by Vogt and collaborators (Vogt, 1993; Vogt *et al.*, 2001; Vogt and Vogt, 2003; Vogt *et al.*, 2003) and shown in Figure 2.1. To enable precise cytoarchitectural identification of cingulate areas, prints of the digitised autoradiographs were superimposed onto the corresponding silver-stained section with a microscope equipped with a drawing tube. The regions drawn on the print were then transferred to the linearized digitized autoradiograph and the mean receptor concentration per unit protein (fmol/mg protein) contained in a specific region over a series of three to five sections was determined. Again here, for a detailed methodological review, see Zilles and collaborators (2002a, 2002b).

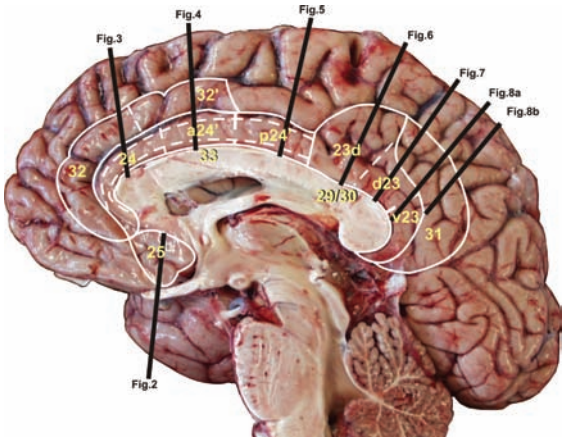

Fig. 2.1 Photograph of the medial surface of a case before freezing with the area borders outlined on the cingulate and paracingulate gyral surfaces. The orientation of sections used in seven subsequent figures is provided along with the figure numbers.

Neurotransmitter Receptor Distribution Patterns

Glutamatergic System

Glutamate is the major excitatory neurotransmitter in the human cerebral cortex and mediates its actions via activation of both ionotropic and metabotropic receptor families. The ionotropic glutamate receptors are ligand-gated ion channels and have been named after the agonists that were originally identified to selectively activate them: α-amino-3-hydroxy-5-methyl-4-isoazolepropionic acid, 2-carboxy-3-carboxymethyl-4-isopropenylpyrrolidine and *N*-methyl-D-aspartate for the AMPA, kainate and NMDA receptors, respectively.

NMDA is the prevailing glutamate receptor subtype in the cingulate cortex. The AMPA receptor displays the

second highest density measured in the anterior cingulate cortex (ACC), whereas the kainate receptor reaches the second place in this ranking in the posterior cingulate cortex (PCC). Thus, the balance between different receptor subtypes for glutamate changes between ACC and PCC. The AMPA and kainate receptors present a clear rostrocaudal gradient with highest concentrations of both receptor types in ACC, intermediate values in the midcingulate cortex (MCC), and lowest densities in PCC. Conversely, lowest NMDA receptor densities were found in ACC (with the exception of area 25), whereas MCC, PCC, and RSC contained comparable densities of this receptor type. Area 25 contains the highest NMDA receptor densities measured in the cingulate cortex. Additionally, the glutamate receptor types are differently distributed in the layers of each area. AMPA and NMDA receptors are characterized by higher concentrations in the supragranular than in the infragranular layers, whereas the opposite holds true for the kainate receptors. A more detailed analysis of the laminar pattern of the AMPA, kainite, and receptors in the cingulate cortex follows below.

The ACC is characterized by higher AMPA and kainate receptor densities when compared to the more posterior cingulate regions (Table 2.1). Thus, under normal conditions ACC areas may work on a higher glutamatergic excitation level via AMPA and kainate receptors than MCC and PCC areas. Additionally, ACC may be more susceptible to pathological processes characterized by hyperexcitation during the early stages (Wenk and Barnes, 2000), since they involve a further shift toward the glutamatergic side of the balance between glutamatergic excitation and GABAergic inhibition. Thus, an effective pharmacologic antagonism of glutamate receptors in general, and of the NMDA receptor in particular, may slow the progression of neurodegenerative diseases such as Alzheimer's disease (Wenk and Barnes, 2000).

TABLE 2.1 Glutamate Receptor Binding Throughout Cingulate Cortex

Area	AMPA	kainate	NMDA
29l	370 ± 104	371 ± 7	1087 ± 56
29m	374 ± 113	385 ± 9	1089 ± 32
30	336 ± 69	414 ± 8	1117 ± 41
33	294 ± 29	253 ± 2	1176 ± 80
25	438 ± 2	424 ± 3	1457 ± 33
24a	500 ± 9	530 ± 80	828 ± 72
a24a′	343 ± 30	325 ± 45	1236 ± 82
p24a′	273 ± 24	436 ± 65	1053 ± 87
24b	488 ± 35	551 ± 26	761 ± 54
a24b′	361 ± 28	370 ± 12	1268 ± 58
p24b′	299 ± 29	466 ± 62	1068 ± 7
24cv	458 ± 15	418 ± 25	722 ± 33
24cd	452 ± 24	375 ± 46	700 ± 26
24c′v	288 ± 44	263 ± 3	1106 ± 29
24c′d	261 ± 35	236 ± 5	1034 ± 43
24dv	246 ± 27	363 ± 45	905 ± 24
24dd	287 ± 71	331 ± 37	876 ± 79
32	413 ± 78	433 ± 46	643 ± 2
32′	323 ± 7	300 ± 10	890 ± 85
23d	368 ± 26	499 ± 11	1225 ± 139
23c	463 ± 201	477 ± 84	1216 ± 18
d23	345 ± 118	378 ± 51	1175 ± 23
v23	307 ± 76	458 ± 19	1145 ± 138
31	385 ± 95	270 ± 250	1187 ± 46

Mean densities (±SD) in fmol/mg protein of the glutamate AMPA, kainate, and NMDA receptors, which were labelled with [^{3}H]AMPA, [^{3}H]kainate, and [^{3}H]MK-801, respectively.

AMPA receptors

The laminar pattern of the AMPA receptors, which we labelled with the agonist [^{3}H]AMPA, is characterized by high densities in the supragranular layers, with a local maximum in layer II and upper layer III, and decreasing concentrations in the infragranular layers. This pattern confirms previous reports concerning not only the cingulate cortex (Jansen *et al.*, 1989), but also other brain regions such as the primary visual and motor cortices (Zilles and Palomero-Gallagher, 2001; Zilles *et al.*, 2002b, 2004). However, some cingulate areas, which will be discussed in detail below, deviate slightly from this pattern, and present local minima or maxima in specific cortical layers. Additionally, AMPA receptor densities are subject to a rostrocaudal gradient within the cingulate cortex, with highest mean densities (averaged over all cortical layers) located rostrally and lowest concentrations in areas 23 and 31.

The laminar pattern of AMPA receptors in area 25 corresponds to the general model described above, with high concentrations in the superficial layers and decreasing values toward the white matter border as shown in Figure 2.2. Mean AMPA receptor densities are lower in area 25 than in area 32 (Table 1). Areas 24a-c and 32 can be delineated from each other based on variations in their AMPA laminar patterns, though they contain comparable mean AMPA receptor densities (Table 2.1). Areas 24a and 24c contain lower AMPA receptor densities in the deep layers than area 24b (Fig. 2.3). Area 32 contains the lowest AMPA receptor density in this ranking. Areas 24b and 32 differ from the general laminar pattern described above for the AMPA receptors. In addition to the high density of

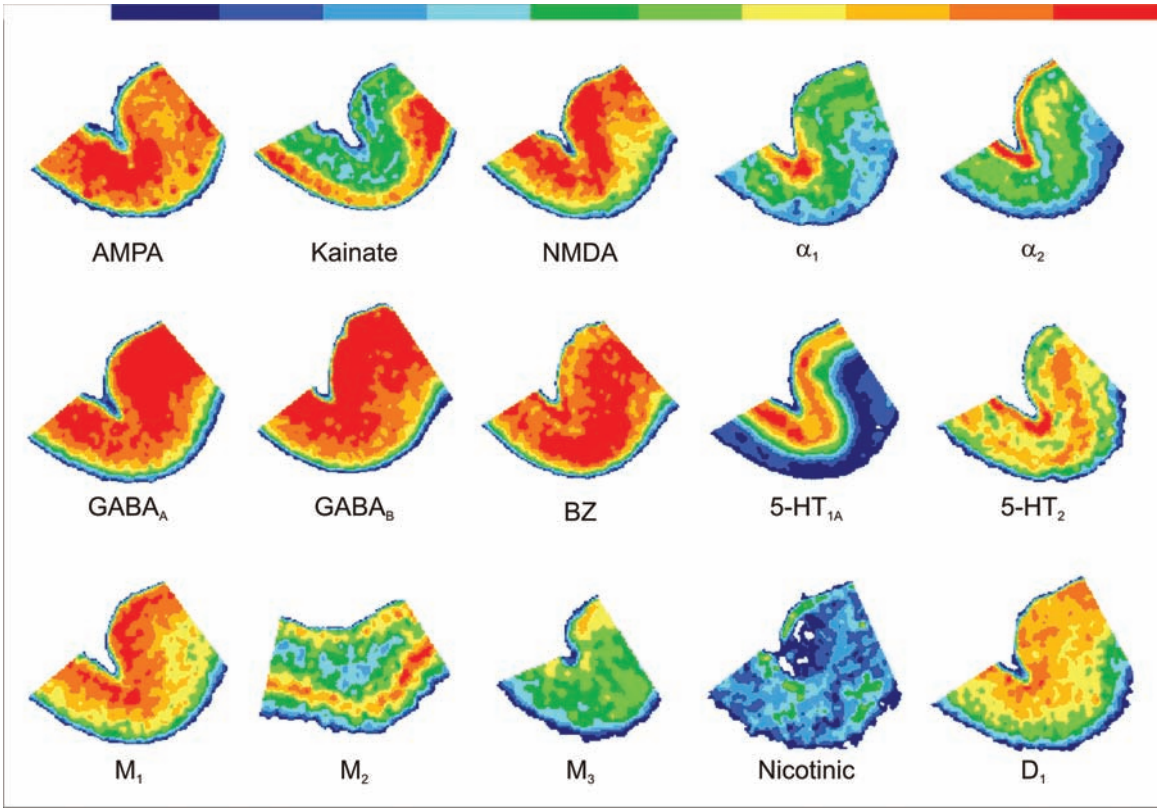

Fig. 2.2 Laminar patterns in area 25. Neighbouring coronal cryostat sections (15µm thick) through a whole human hemisphere were processed for the visualisation of glutamate (AMPA, kainate, NMDA), GABA ($GABA_A$, $GABA_B$, benzodiazepine binding sites), acetylcholine (muscarinic M_1, M_2, M_3, and nicotinic), noradrenaline (α_1, α_2), serotonin ($5\text{-}HT_{1A}$, $5\text{-}HT_2$), and dopamine (D_1) receptors. Colour coding of the scale bar indicates binding site densities in fmol/mg protein. Each section was individually contrast enhanced in order to most clearly display laminar distribution pattern and is oriented in such a way that the pial surface is at the top of the image and the white matter border at the bottom.

AMPA receptors in the superficial layers, these two regions are characterized by a local maximum in layer Vb, which is flanked by local minima in layers Va and VI (Fig. 2.3). This local maximum is particularly pronounced in area 24b. Periallocortical area 33 contains lower concentrations than area 24a, but higher values than those measured in a24a′ or p24a′ (Fig. 2.3).

Anterior midcingulate areas a24a′-b′, 24c′, and 32′ contain lower AMPA receptor densities than areas 24a-c and 32 (Table 2.1), but higher concentrations than those measured in areas p24a′-b′ and 24d (Table 2.1). The infragranular layers of area a24a′ contain higher AMPA receptor densities than those of a24b′ (Fig. 2.4). In area a24b′ AMPA densities are clearly higher in the superficial than in the deep layers, and layer Vb shows a relative maximum. In area 24c′, layer IIIc presents a local minimum, thus clearly visualizing the border between both areas. The laminar pattern of the AMPA receptors in area 32′ is comparable to that described for 24c′.

The laminar pattern of AMPA receptors in posterior midcingulate p24a′-b′ and 24dd is characterized by high densities in the superficial layers, with values decreasing toward layer VI, and a less pronounced local maximum in layer Vb of p24b′ (Fig. 2.5). Areas p24a′ and 24dv contain lower AMPA concentrations than p24b′ particularly in the supragranular layers. Areas 24dv and 24dd do not differ significantly in their AMPA receptor densities or laminar patterns.

Posterior cingulate area 23d contains a higher concentration of AMPA receptors than areas d23 and v23 and the adjoining periallocortical regions (Table 2.1). All subdivisions of area 23 present a local maximum in layer Vb (Figs. 2.6–2.8). Although similar concentrations of AMPA receptors were measured in areas v23 and 31 (Table 2.1), they can be distinguished from each other due to the fact that the local maximum in layer Vb of area v23 is more pronounced than that of area 31 (Fig. 2.8).

The retrosplenial cingulate areas differ from the adjacent isocortical areas in their mean AMPA receptor

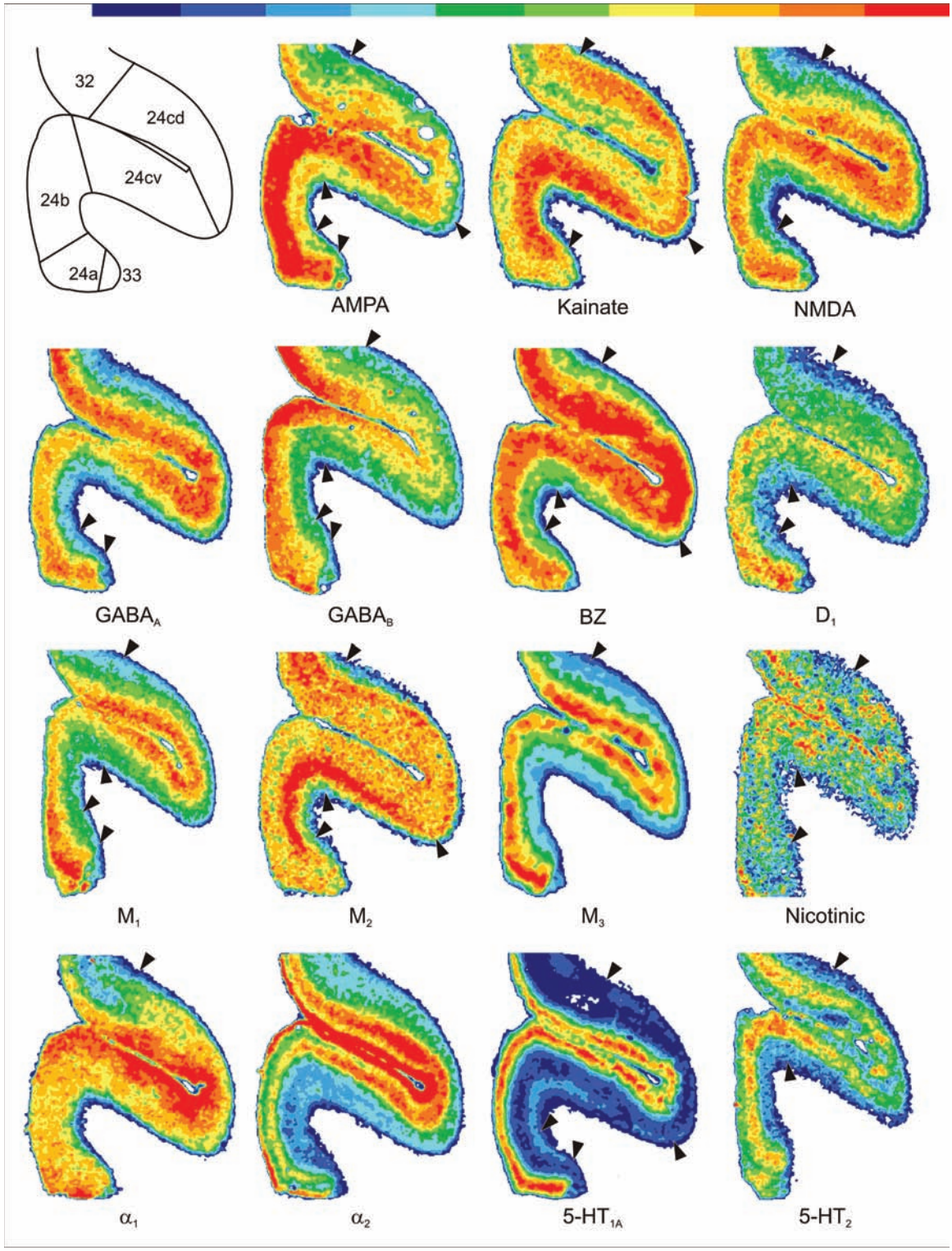

Fig. 2.3 Laminar patterns in anterior cingulate cortical areas. Each section was individually contrast enhanced in order to most clearly display interareal borders present in the depicted rostrocaudal level.

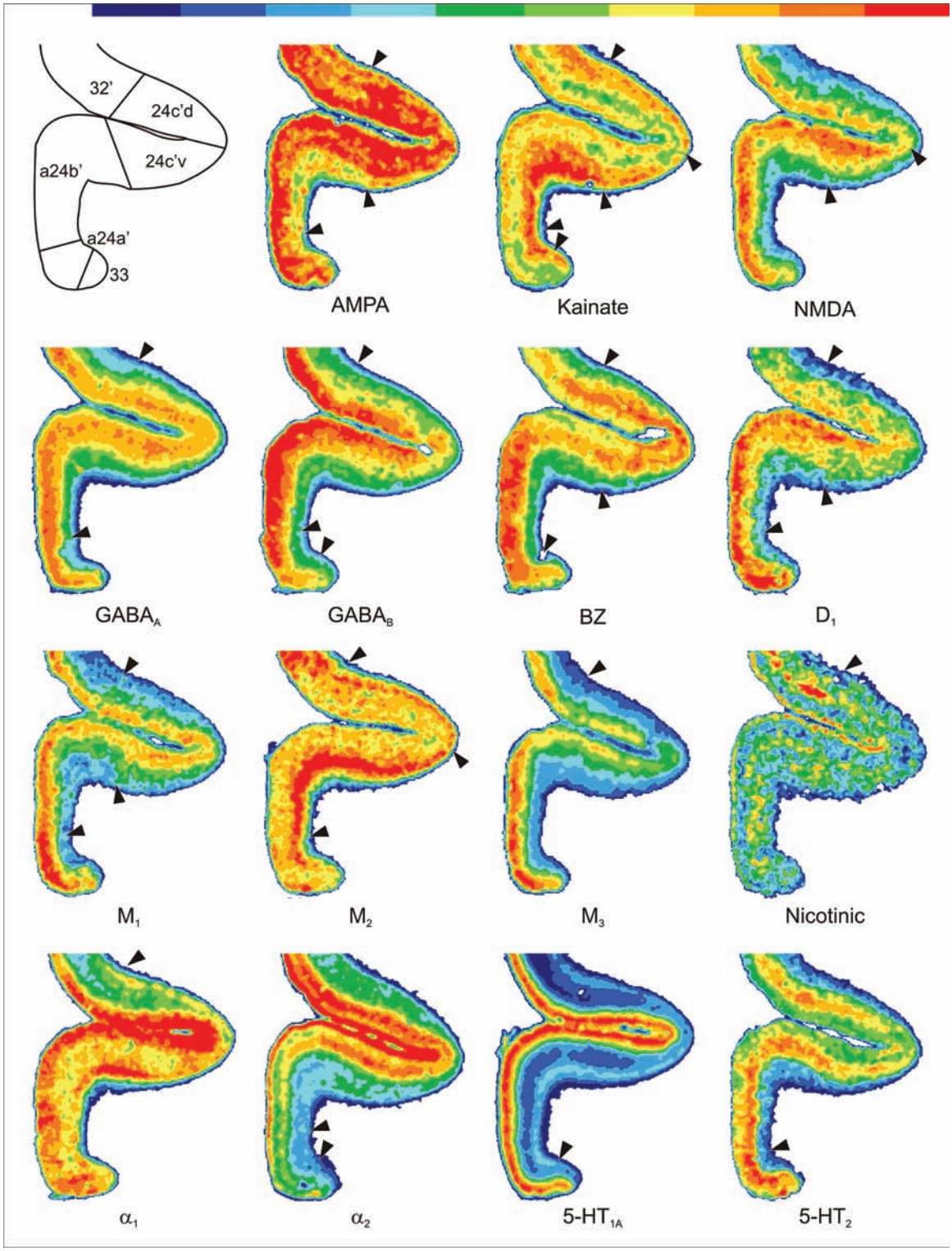

Fig. 2.4 Laminar patterns in anterior midcingulate cortical areas.

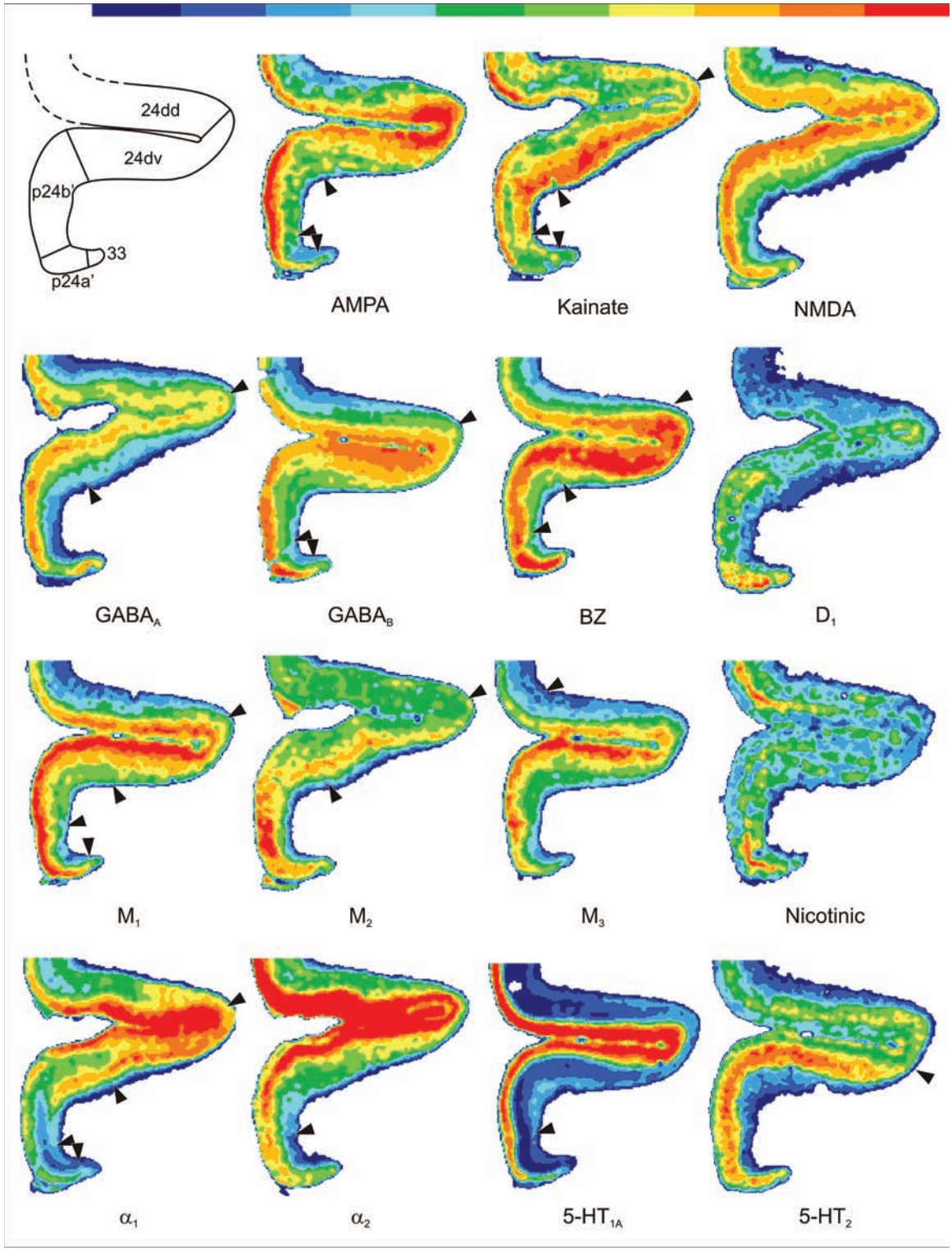

Fig. 2.5 Laminar patterns in posterior midcingulate cortical areas.

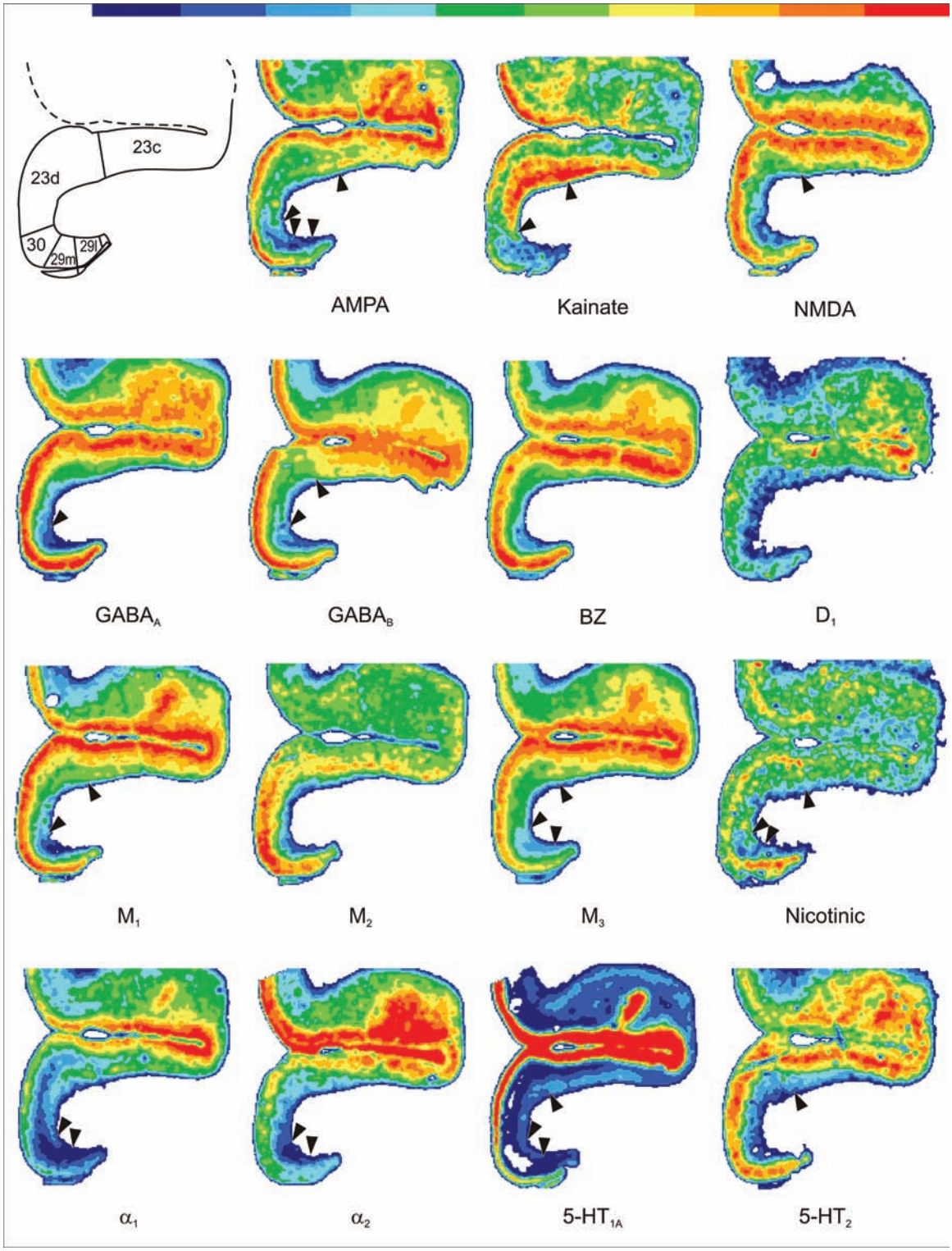

Fig. 2.6 Laminar patterns in dorsal posterior cingulate cortical areas 23d and 23c and in the retrosplenial cortex.

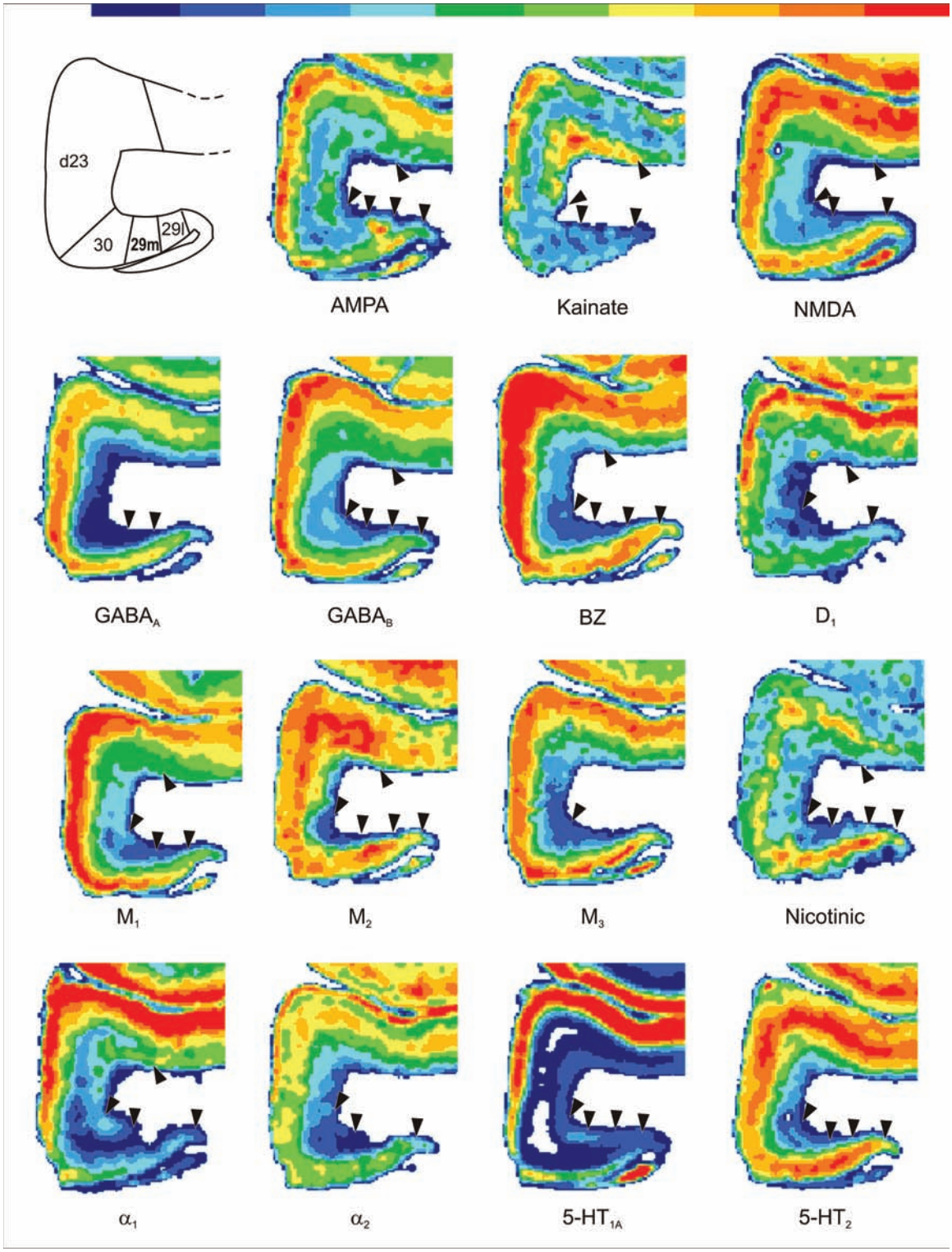

Fig. 2.7 Laminar patterns in dorsal posterior cingulate cortical area d23 and in the retrosplenial cortex.

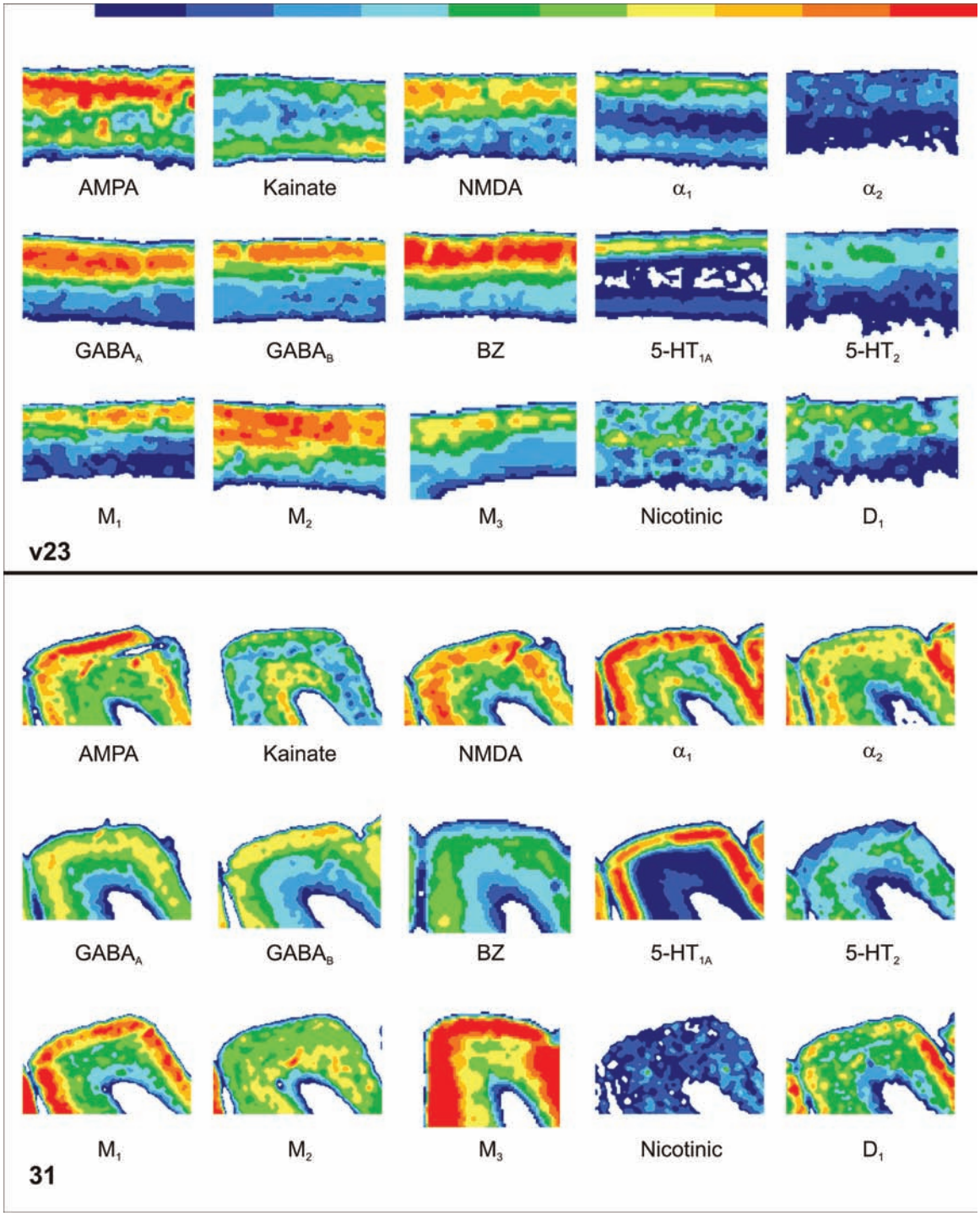

Fig. 2.8 Laminar patterns in posterior cingulate cortical areas v23 and 31. Sections are oriented in such a way that the pial surface is at the top of the image and the white matter border at the bottom.

densities (Table 2.1). The infragranular layers of area 30 contain lower AMPA receptor densities than those of area d23 (Fig. 2.7). Areas 29 and 30 can be distinguished due to the higher AMPA receptor densities in the upper layers of area 30 (Fig. 2.7). The deeper layers of area 29l contain higher AMPA receptor densities than those of area 29m.

Kainate receptors

Kainate receptors were labelled with the agonist [^{3}H]kainate. Their laminar pattern differs significantly from that of the AMPA and NMDA receptors. The isocortical areas of the cingulate cortex present a differentiated laminar pattern, as described previously for the cingulate cortex and other cortical regions (Jansen *et al*., 1989; Zilles and Palomero-Gallagher, 2001; Zilles *et al*., 2003, 2004): high kainate receptor densities in layers I-II and V-VI are interleaved with low densities in layer(s) III (and IV). The relatively highest kainate binding site densities are located in layers V-VI. This specific laminar pattern of the kainate receptor is in accordance with the distribution of kainate receptor subunits and/or their encoding mRNAs, since a GluR 5/6/7 antibody (Vickers *et al*., 1995) and the GluR7 transcript (Porter *et al*., 1997) have been demonstrated to prevail in layers V-VI and to be less dense in the superficial layers. Conversely, the GluR6 subunit and KA2 mRNAs are found not only in layers II-III, but also in layers V-VI (Porter *et al*., 1997). The absolute kainate receptor densities present a rostrocaudal gradient within the cingulate cortex, with highest kainate concentrations located rostrally (Table 2.1).

Anterior cingulate area 25 contains clearly higher kainate receptor densities in the deep than in the superficial layers (Fig. 2.2). Furthermore, the concentration of kainate receptors in layer II is only slightly higher than that seen in layers III-IV. Areas 24a-c differ in their laminar patterns (Fig. 2.3). Area 24b shows clearly lower densities in layer III than area 24a, but slightly higher concentrations than area 24c. Layer III of area 32 contains considerably lower kainate receptor densities than that of area 24c. Periallocortical area 33 exhibits a simple laminar pattern, with lowest densities in the deeper cortical layers and increasing concentrations are found toward the pial surface (Fig. 2.3).

A new finding is the fact that kainate receptors are heterogeneously distributed throughout area 24c (Fig. 2.3). Therefore, it is possible to establish a border located in the fundus of the cingulate sulcus which separates a ventral subdivision (24cv, located on the ventral bank of the cingulate sulcus) from a dorsal subdivision (24cd, located on the dorsal bank of the cingulate sulcus) of area 24c. The deep layers of 24cv contain a higher kainate receptor density than those of 24cd. This distinction has not been previously made in cytoarchitectural studies. Specific cytoarchitecture indicates a single area located within the cingulate sulcus.

Anterior midcingulate areas a24a′-b′, 24c′, and 32′ can be distinguished from areas of ACC due to the clearly lower kainate receptor densities measured in the former regions (Table 2.1) as well as due to differences in their laminar patterns. Whereas layer III of area 24a contains higher kainate densities than that of area 24b (Fig. 2.3), the opposite constellation is observed between areas a24a′ and a24b′ (Fig. 2.4). Layer III of area 24c′ contains clearly lower kainate receptor densities than that of area a24b′ (Fig. 2.4).

Following the above described trend set by the rostrocaudal gradient in mean absolute kainate receptor densities, posterior midcingulate areas p24a′-b′ and 24d present clearly lower mean concentrations than those measured in a24a′-b′ and 24c′ (Table 2.1). Furthermore, the dorsal part of area 24d (24dd) contains lower kainate receptor densities than its ventral counterpart (24dv, Fig. 2.5), particularly in the deep layers. This differential distribution of the kainate receptors within area 24d suggests that the dorsal and ventral parts of the caudal cingulate motor area are differently regulated by glutamate. This is particularly true for the deep layers, which make spinal projections, and contain highest kainate receptor densities. The border between p24a′ and p24b′ is distinctly visible due to the lower kainate receptor densities in the former area (Fig. 2.5).

The mean kainate receptor density of posterior cingulate area 23d is comparable to that measured in the p24′. It is significantly higher than the values obtained for d23, and slightly higher than the concentration measured in v23 (Table 2.1). Within area 31, the infragranular layers present considerably higher kainate concentrations than the supragranular layers (Fig. 2.8).

In the retrosplenial areas, kainate binding sites exhibit a simple laminar pattern and show the borders between areas 30 and 23 (Fig. 2.7). Highest kainate receptor density of areas 29 and 30 is in the upper cortical layers and kainate receptor concentrations decrease in the deeper layers (Fig. 2.7). Neither differences in the mean kainate receptor densities nor in their laminar patterns enable the definition of the border between areas 29 and 30 or the differentiation of area 29 into its lateral and medial parts (Fig. 2.7).

NMDA receptors

The laminar pattern of the NMDA receptors, which were labelled with the antagonist [^{3}H]MK-801, remains constant in both the isocortical and periallocortical cingulate regions: maxima are seen in the superficial cortical layers and decreasing densities are found in the deeper layers. This laminar pattern is in accordance

with that previously described for the cingulate, visual, and motor cortices (Jansen *et al.*, 1989; Zilles *et al.*, 2002b, 2003, 2004). In contrast to the situation described for AMPA and kainate receptors, NMDA receptors are present in lowest densities in ACC (Table 2.1).

Anterior cingulate area 25 can be clearly delineated from area 32 due to its significantly higher overall NMDA receptor density (Table 2.1). On the other hand, differences between areas 24a-c, 32, and 33 are restricted to their deep NMDA receptor densities. Layers V-VI of areas 24b and 32 contain lower concentrations of NMDA receptors than that of areas 24a or 24c (Fig. 2.3). Periallocortical area 33 contains clearly lower NMDA receptor densities than the adjacent 24a (Fig. 2.3).

Anterior midcingulate areas a24a´-b´, 24c´, and 32´ contain considerably higher NMDA receptor densities than any of the rostrally adjacent areas (Table 2.1). Areas a24a´-b´ and 24c´ do not differ significantly in their mean NMDA receptor densities, and show slightly higher concentrations than area 32´ (Fig. 2.4). Therefore, although NMDA receptors reveal the border between areas 24 and 32´, they do not enable the visualization of the borders between the subdivisions of area 24 at this level.

Posterior midcingulate areas p24a´-b´, 24dv, and 24dd contain higher NMDA receptor densities than a24a´-b´ or 24c´ (Table 2.1). However, the NMDA receptors do not enable the visualization of the borders between the subdivisions of area 24 at this rostrocaudal level either (Fig. 2.5).

Area 23d contains higher NMDA receptor densities than either d23 or v23 (Table 2.1). Area 31 and d23 show comparable NMDA receptor densities, and area v23 presents only slightly lower concentration of NMDA receptors than d23 or 31 (Table 2.1).

Retrosplenial areas 29 and 30 present comparable NMDA receptor densities, which are lower than those measured in area 23d (Fig. 2.7). Furthermore, the NMDA receptors are homogeneously distributed within 29 and, therefore, do not visualize the subdivision of this area into its lateral and medial parts (Fig. 2.7).

GABAergic System

GABA receptors have traditionally been classified into three groups, $GABA_A$, $GABA_B$, and $GABA_C$ on the basis of their pharmacological profiles. We examined the distribution of $GABA_A$ and $GABA_B$ receptors as well as of the $GABA_A$ associated benzodiazepine (BZ) binding sites in the cingulate cortex. The $GABA_A$ receptors had the lowest mean concentrations and BZ the highest densities of the three examined types of GABA binding sites (Table 2.2). $GABA_A$ receptors and BZ binding sites are present in higher concentrations in PCC than in ACC or MCC. Conversely, $GABA_B$ receptor densities are comparable in most areas of ACC and PCC. The BZ binding sites prevail over $GABA_B$ receptors in PCC. The laminar pattern of the $GABA_A$ and $GABA_B$ receptors as well as BZ binding sites does not change along the rostrocadal axis. All three subtypes show clearly higher densities in the supragranular than in the infragranular layers of the cingulate cortex (with the exception of area 25, which will be discussed bellow).

The balance between different GABA receptor subtypes changes along the rostrocaudal axis of the cingulate cortex. The PCC is characterized by higher densities of $GABA_A$ and BZ binding site densities when compared to ACC and MCC. Additionally, PCC contains higher $GABA_B$ receptor densities than MCC. Therefore, under

TABLE 2.2 GABA Receptor Ligand Binding Throughout Cingulate Cortex

Area	$GABA_A$	$GABA_B$	BZ
29l	1916 ± 390	2054 ± 99	2955 ± 355
29m	1788 ± 150	2097 ± 177	3035 ± 425
30	1785 ± 60	2232 ± 145	3167 ± 573
33	1090 ± 62	1012 ± 99	1278 ± 97
25	1315 ± 47	1140 ± 30	1406 ± 47
24a	624 ± 213	2163 ± 14	1826 ± 203
a24a´	1158 ± 38	1042 ± 87	1364 ± 242
p24a´	1246 ± 68	1863 ± 89	2082 ± 35
24b	631 ± 163	2268 ± 132	1909 ± 122
a24b´	1119 ± 17	1046 ± 131	1348 ± 90
p24b´	1260 ± 60	1973 ± 150	1991 ± 10
24cv	567 ± 150	1977 ± 109	1888 ± 136
24cd	642 ± 233	1897 ± 13	1966 ± 142
24c´v	1242 ± 46	1042 ± 93	1358 ± 75
24c´d	1218 ± 22	989 ± 121	1306 ± 60
24dv	1196 ± 25	1724 ± 95	1927 ± 182
24dd	1283 ± 43	1736 ± 37	1837 ± 96
32	732 ± 59	2060 ± 140	1911 ± 18
32´	1011 ± 25	882 ± 68	1335 ± 64
23d	1700 ± 3	2396 ± 300	3080 ± 347
23c	1769 ± 133	2372 ± 1	2610 ± 168
d23	1585 ± 27	1587 ± 130	2906 ± 557
v23	1866 ± 95	1022 ± 41	3195 ± 7
31	1921 ± 116	1941 ± 201	1941 ± 83

Mean densities (±SD) in fmol/mg protein of the $GABA_A$ and $GABA_B$ receptors as well as of the $GABA_A$ associated benzodiazepine (BZ) binding sites, which were labelled with [^{3}H]muscimol, [^{3}H]CGP54626, and [^{3}H]flumazenil, respectively.

normal physiological conditions, PCC areas work on a higher GABAergic inhibition level than the ACC and MCC regions do. Thus, activation mediated by the glutamatergic system is balanced by fast intrinsic GABAergic inhibition more rapidly in PCC than in ACC.

Diseases that impact the cingulate cortex are often associated with altered GABAergic function. Reductions in the levels of BZ binding site densities have been shown in panic disorder (Malizia *et al*., 1998; Nutt and Malizia, 2001). This suggests a lower GABAergic inhibition of PCC under pathological conditions. Thus, PCC in general terms, and its supragranular layers in particular, may be the site of GABAergic transmission involved in the prompt actions of anxyolitic drugs.

$GABA_A$ receptors and $GABA_A$ associated BZ sites

The ionotropic $GABA_A$ receptor was labelled with its agonist [^{3}H]muscimol. Mean $GABA_A$ receptor densities (averaged over all cortical layers) are lower in ACC (excepting area 25) than in MCC and PCC (Table 2.2). Additionally, $GABA_A$ receptor densities are significantly higher in the supragranular than in the infragranular layers of the cingulate cortex. Furthermore, when present, layer IV contained clearly higher $GABA_A$ receptor densities than layers V or VI. This laminar pattern coincides with that described previously for area 23a and for other cortical regions (Rakic *et al*., 1988; Vogt *et al*., 1990, 1991, Vogt 1992; Zilles *et al*., 2002a, 2002b, 2004), and is also in accordance with the localization of the $GABA_A$ receptors within the limits of terminal fields of GABAergic axons and synapses, and with the layer-specific distribution of the $GABA_A$ receptor subunits α1, α2/3, and α2 (Hendry *et al*., 1994).

The $GABA_A$ associated BZ sites were labelled with [^{3}H]flumazenil, an antagonist frequently used in receptor-positron emission tomography (PET) studies. The laminar pattern of the BZ binding sites is characterized, with the exception of area 25, by high densities in the supragranular layers, with a local maximum in the supragranular and granular (when present) layers, and lower concentrations in the infragranular layers. This pattern is the same as that described above for the $GABA_A$ receptors. The BZ binding site densities are clearly higher than $GABA_A$ receptor densities, reflecting the fact that a single $GABA_A$ receptor may have more than one BZ binding site (Araujo *et al*., 1996).

Anterior cingulate area 25 contains clearly higher $GABA_A$ receptor densities but lower BZ binding site densities than area 32 (Table 2.2). As mentioned above, the laminar pattern of BZ binding site densities in area 25 differs from that observed in the remaining cingulate areas. BZ binding sites increase throughout the supragranular layers, reach a local maximum in layers IIIc-IV, and decrease again in the infragranular layers, reaching lowest values at the white matter border. Thus, area 25 can be clearly distinguished from area 32 (Table 2.2).

Areas 24a-c and 32 do not differ significantly in their mean $GABA_A$ receptor or BZ binding site densities. However, layer IIIc of area 24b contains lower $GABA_A$ receptor densities than the areas 24a or 24c (Fig. 2.3). Additionally, the superficial layers of area 24a present slightly lower BZ binding site densities than those of area 24b (Fig. 2.3). The deep layers of 24b contain lower BZ binding site concentrations than those of area 24c. The BZ binding sites also enable the subdivision of area 24c into a dorsal and a ventral component (as described above for the kainate receptors). Area 24cv contains lower BZ binding site densities than 24cd (Fig. 2.3). A lower $GABA_A$ receptor density in layer IIIc of area 32 also serves as a marker to determine its border with 24c (Fig. 2.3).

Anterior midcingulate areas a24a´-b´, 24c´, and 32´ contain higher $GABA_A$ receptor but lower BZ binding site densities than 24a-c or 32 (Table 2.2). Area a24b´ shows slightly higher $GABA_A$ receptor densities than a24a´, particularly in the deep layers, but lower values than those seen in 24c´ (Fig. 2.4). Area a24b´ can be clearly delineated from areas a24a´ and 24c´ due to its higher BZ binding site densities, particularly in the superficial layers (Fig. 2.4). As was the case between areas 24c and 32, the border between 24c´ and 32´ is made evident by a reduction of the $GABA_A$ receptor and BZ binding site densities in layer IIIc of the latter area (Fig. 2.4).

Posterior midcingulate areas p24a´-b´, 24dv, and 24dd (Table 2.2) contain comparable $GABA_A$ receptor densities to those measured in the rostrally adjacent areas, but slightly higher BZ binding site densities. These areas do not differ in their mean $GABA_A$ receptor or BZ binding site densities. However, the border between p24a´ and p24b´ can be defined based on the lower concentrations of BZ binding sites present in p24b´ (Fig. 2.5). Areas p24b´ and 24dv can be distinguished since area p24b´ contains higher superficial but lower deep concentrations than area 24dv. Additionally, p24b´ contains lower deep of BZ binding sites than 24dv. Areas 24dv and 24dd can be differentiated based on the slightly lower BZ binding site densities in the latter area (Fig. 2.5).

Posterior cingulate area 23 contains higher $GABA_A$ and BZ binding site densities than ACC or MCC (Table 2.2). Within area 23, lowest $GABA_A$ densities were measured in d23, whereas 23c contained lowest BZ binding site densities. Mean $GABA_A$ receptor densities in area 31 are comparable to those of area v23, and higher than the concentrations measured in d23 (Table 2.2). On the other hand, area 31 contains clearly lower BZ binding site densities than either d23 or v23. Areas 23d and 23c do not differ in their $GABA_A$ receptor

densities, but area 23d contains higher BZ binding site densities than area 23c (Table 2).

$GABA_A$ receptor concentrations and BZ binding site densities measured in retrosplenial areas 29 and 30 are comparable to those in area 23 (Table 2.2). Areas 29 and 30 can be distinguished due to the overall higher $GABA_A$ receptor densities in area 29 and to the lower BZ densities in the superficial layers of area 30 (Fig. 2.7). Both the $GABA_A$ receptors and the BZ binding sites visualize the border between the lateral and medial subdivisions of area 29. The lateral part contains slightly lower $GABA_A$ receptor densities in the upper layers than the medial subdivision (Fig. 2.7). Furthermore, area 29l contains higher BZ binding site densities in layer V than area 29m (Fig. 2.7).

$GABA_B$ receptors

The metabotropic $GABA_B$ receptors were visualized with the antagonist [^{3}H]CGP 54626. The laminar pattern of the $GABA_B$ receptors is characterized by high densities in the supragranular layers, with a local maximum in layers II-III, and much lower concentrations in the infragranular layers. This pattern is similar to that described for other regions of the human cerebral cortex (Chu *et al.*, 1987; Zilles *et al.*, 2004). $GABA_B$ receptor densities do not show a clear rostrocaudal gradient within the cingulate cortex. They are present in lowest concentrations in the anterior MCC (aMCC) and in areas 25, v23, and 33 (Table 2.2).

Anterior cingulate area 24a contains slightly higher $GABA_B$ receptor densities in the deep layers than 24b (Fig. 2.3). Area 24c contains lower $GABA_B$ receptor densities than areas 24b or 32 (Table 2.2, Fig. 2.3). This difference is especially evident in the superficial layers. Periallocortical area 33 contains lower $GABA_B$ receptor densities than area 24a (Table 2.2).

Anterior midcingulate areas a24a′, a24b′, 24c′, and 32′ contain clearly lower mean $GABA_B$ densities than the rostrally or caudally adjacent areas. Areas a24b′, 24c′, and 32′ can be distinguished based on the concentration of $GABA_B$ receptors in their layer IIIc: highest relative values are in area a24b′ and the lowest densities are in layer IIIc of area 32′ (Fig. 2.4).

The density of $GABA_B$ receptors is considerably higher in the posterior MCC (pMCC) than in aMCC (Table 2.2). Area p24a′ contains lower $GABA_B$ receptor densities in the deep layers than area p24b′ (Fig. 2.5). Layers IIIc-VI of area 24dv contain a higher concentration of $GABA_B$ receptors than those of areas p24b′ or 24dd (Fig. 2.5).

Posterior cingulate areas 23 and 31 are characterized in general terms by a maximum of $GABA_B$ receptors in layer II and upper layer III, followed by a decrease in layer IIIc, and lowest concentrations in the infragranular layers (Figs. 2.6-2.8). Areas 23d, d23, and 31 do not differ in their mean $GABA_B$ receptor densities, which are slightly higher than those measured in area v23 (Table 2.2).

Mean $GABA_B$ receptor densities are lower in retrosplenial areas 29 and 30 than in the adjacent isocortical regions. Areas 29 and 30 can be distinguished due to the higher $GABA_B$ receptor densities in the superficial layers of the latter area (Fig. 2.7). However, $GABA_B$ receptors do not visualize the border between the lateral and medial parts of area 29 (Fig. 2.7).

Cholinergic System

Acetylcholine receptors are classified as nicotinic and muscarinic subtypes and play a modulatory role in the central nervous system by enhancing signal-to-noise ratios in cortical target areas (Alcantara *et al.*, 2001; de Rover *et al.*, 2004). We examined the distribution of neuronal α_4/β_2 and α_3 nicotinic (N) receptors in the cingulate cortex and of muscarinic M_1, M_2, and M_3 receptors. Nicotinic receptors are in considerably lower densities than muscarinic receptors of any class, which is in agreement with previous observations in other human cortical areas (Zilles *et al.*, 2002a, 2002b, 2004). Binding to M_3 receptors is highest in cingulate cortex, M_1 binding is intermediate, whereas M_2 binding is lowest.

Nicotinic receptors present a clear rostrocaudal gradient in mean densities in cingulate cortex. Lowest nicotinic receptor densities were measured in ACC and highest values were found in PCC and RSC (Table 2.3). Although mean densities of the muscarinic M_1, M_2, and M_3 receptors did not show clear rostrocaudal gradients, areas of PCC contained higher densities than those of ACC (Table 2.3). This gradual increase in muscarinic receptor densities in the rostral-to-caudal cingulate areas goes hand in hand with an increase of the GABA receptor densities but a decrease of the glutamate AMPA and kainate receptor densities. Thus, excitatory neurotransmission in PCC is not only more strongly countered by GABA inhibition than in ACC, but it is also subject to a stronger modulation via the cholinergic system. Therefore, the more subtle activations reported for PCC may be due to this complex interplay of modulatory processes.

Muscarinic M_1 and M_3 receptors

Muscarinic M_1 and M_3 receptors were visualized with the antagonists [^{3}H]pirenzepine and [^{3}H]4-DAMP, respectively. Since the laminar patterns of M_1 and M_3 receptors are similar, they are described here together. They are characterized by high densities in the supragranular layers, with a local maximum in layers II-III, and lower concentrations in the infragranular layers. This pattern is similar to that described for the M_1 receptors in area 23a (Vogt *et al.*, 1990, 1991) and in

other regions of the human cerebral cortex (Rodriguez-Puertas *et al*., 1997; Zilles *et al*., 2004). The distribution pattern of the pyramidal cell bodies labelled by the subtype non-selective muscarinic receptor antibody M-35 (Schröder *et al*., 1989; van der Zee and Luiten, 1999) also reflects the laminar pattern of the M_1 and M_3 receptors.

Anterior cingulate area 32 contains higher M_1 receptor densities than area 25 (Table 2.3). However, these two areas do not differ in their mean M_3 receptor densities. Areas 24a-c show higher M_1 receptor densities than a24a´-b´ and 24c´, but comparable M_3 receptor concentrations (Table 2.3). Area 32 contains higher M_1 and lower M_3 receptor densities than area 32´. The supragranular layers of area 24b have lower M_1 receptor densities than those of 24a or 24c (Fig. 2.3). Supragranular layers of area 32 have lower M_1 and M_3 receptor densities than in area 24c. One of the critical issues in receptor architecture is the extent to which the distribution of a given receptor type reveals all areal borders. The M_3 receptors do not reveal the a-c subdivisions of area 24. However, they do show the borders between area 24 and areas 33 and 32 (Fig. 2.3). Periallocortical area 33 contains one of the lowest M_1 and M_3 receptor densities measured within the cingulate cortex (Table 2.3).

The superficial layers of anterior midcingulate area a24a´ have higher M_1 receptor densities than those of a24b´ (Fig. 2.4). The deep layers of 24c´ contain higher M_1 receptor densities than those of a24b´ (Fig. 2.4). Areas a24a´ and a24b´ cannot be distinguished based on the M_3 receptor distribution patterns (Fig. 2.4). Area 24c´ contains lower M_3 receptor densities in the superficial layers than either a24b´ or 32´ (Fig. 2.4). Area 32´ contains lower M_1 but higher M_3 receptor densities than area 24c´ (Fig. 2.4).

Posterior midcingulate areas p24a´-b´ and 24d contain clearly higher M_1 receptor densities than areas a24a´-b´ or 24c´, but comparable M_3 receptor

TABLE 2.3 Acetylcholine Receptors Throughout Cingulate Cortex

	M_1	M_2	M_3	Nicotinic
29l	431 ± 31	180 ± 6	1015 ± 7	117 ± 4
29m	446 ± 23	178 ± 12	962 ± 7	105 ± 7
30	525 ± 14	172 ± 3	872 ± 7	95 ± 11
33	242 ± 25	124 ± 32	499 ± 8	41 ± 12
25	359 ± 38	160 ± 14	595 ± 50	28 ± 2
24a	499 ± 109	132 ± 14	566 ± 52	32 ± 6
a24a´	261 ± 27	142 ± 27	498 ± 13	44 ± 10
p24a´	577 ± 1	122 ± 5	546 ± 19	39 ± 2
24b	454 ± 30	136 ± 1	533 ± 6	33 ± 2
a24b´	300 ± 29	154 ± 19	458 ± 10	42 ± 3
p24b´	576 ± 29	135 ± 4	526 ± 23	35 ± 6
24cv	397 ± 91	116 ± 5	523 ± 12	32 ± 1
24cd	387 ± 108	103 ± 6	545 ± 24	33 ± 1
24c´v	295 ± 11	145 ± 10	468 ± 5	50 ± 8
24c´d	302 ± 13	147 ± 13	462 ± 1	45 ± 15
24dv	447 ± 71	109 ± 8	500 ± 46	39 ± 8
24dd	406 ± 41	112 ± 2	486 ± 20	44 ± 9
32	479 ± 46	128 ± 1	583 ± 15	39 ± 1
32´	226 ± 24	496 ± 22	796 ± 23	62 ± 5
23d	581 ± 65	164 ± 1	632 ± 7	82 ± 1
23c	486 ± 9	152 ± 20	667 ± 7	74 ± 15
d23	596 ± 4	179 ± 7	615 ± 21	80 ± 28
v23	606 ± 58	189 ± 27	531 ± 1	73 ± 15
31	681 ± 168	196 ± 65	560 ± 66	86 ± 10

Mean densities (±SD) in fmol/mg protein of the muscarinic M_1, M_2, and M_3 as well as of the nicotinic receptors, which were labelled with [^{3}H]pirenzepine, [^{3}H]oxotremorine-M, [^{3}H]4-DAMP, and [^{3}H]epibatidine, respectively.

concentrations (Table 2.3). Area p24b´ contains higher deep M_1 receptor concentrations than area p24a´ (Fig. 2.5). These two areas do not differ in their mean M_3 receptor densities or laminar patterns. The M_1 and M_3 receptors contribute to another continuing theme of this work. And that is, that area 24d has a dorsal and ventral division lining the cingulate sulcus. Thus, area 24dd contains lower M_1 and M_3 receptor densities than area 24dv (Fig. 2.5).

As a general rule, PCC areas have higher M_1 receptor densities than ACC or MCC areas. Areas 23d, d23, and v23 do not differ in their laminar patterns or in their mean M_1 receptor densities, which are higher than those measured in 23c (Table 2.3; Figs. 2.6 and 2.7). Areas 31 and v23 contain equivalent concentrations of the M_3 receptor, which are lower than those measured among areas 23d, 23c, and d23 (Table 2.3).

Retrosplenial areas 29 and 30 contain the highest M_3 receptor densities of the cingulate cortex. Area 29 contains higher M_1 but lower M_3 receptor densities than area 30 (Table 2.3). The M_1 and M_3 receptors doe not distinguish between the lateral and medial subdivisions of area 29 (Fig. 2.7). This implies that the role of RSC in working memory is significantly mediated by cholinergic innervation.

Muscarinic M_2 receptors

Muscarinic M_2 receptors were labelled with the agonist [^{3}H]oxotremorine-M. Cingulate areas differ only slightly in their mean M_2 receptor densities (averaged over all cortical layers, Table 2.3), but present considerable differences in their laminar patterns, a fact which has also been described in other parts of the human brain (Zilles and Palomero-Gallagher, 2001; Zilles *et al.*, 2002a, 2002b; Scheperjans *et al.*, 2005). Thus, a fascinating characteristic of the M_2 receptor is its ability to differentiate cholinergic control of input and output systems in the cingulate cortex. Cingulate areas can be divided into four groups based on their M_2 laminar patterns:

- In some areas (e.g. p24a', p24b', 23d, d23, v23, 30), M_2 receptors have a bilaminar distribution with highest densities in the supragranular layers and a local maximum in layer III. Vogt and colleagues (1990, 1992) examined the laminar pattern of M_2 receptors in area 23a (a subdivision of our areas d23 and v23) and also reported higher densities in the supragranular than in the infragranular layers.
- Other areas (e.g. a24b', 24c'v, 24c'd, 24dv, 31) show the opposite situation, with highest concentrations in the infragranular layers. The latter laminar pattern partially reflects the localization of choline acetyltransferase-immunoreactive fibres, which are concentrated in layer I, less intense in the middle layers, and increase again in deep layer IV and V.
- A third group of regions (e.g. a24a', 24b, 24cv, 25, 32, 32') presents a laminar pattern composed of alternating minima and maxima.
- In a fourth group of regions, M_2 receptors are homogeneously distributed throughout all layers (e.g. 24a, 24cd, 24dd, 23c, 29l, 29m, 33).

Anterior cingulate area 25 contains higher M_2 receptor densities than areas 24 or 32 (Table 2.3). It has alternating bands of high and low M_2 receptor densities, with a first local maximum in layer II and a second, higher one, in layer Vb (Fig. 2.2). Conversely, M_2 receptors are relatively homogeneous through all layers of area 24a (Fig. 2.3). In area 24b, M_2 receptors are present in intermediate concentrations in layers I-II, followed by a local minimum in layer III and an absolute maximum in layer V (Fig. 2.3). Area 32 contains higher mean M_2 receptor densities than area 24cd (Table 2.3). Additionally, there are considerable differences in their laminar patterns. Area 32 presents high M_2 receptors in layers III and V separated by lower concentrations in layers I-II, IV, and VI (Fig. 2.3).

Although the dorsal and ventral parts of the cingulate sulcus have been separated on the basis of cytoachitecture, receptor-architecture and connectivity in MCC, nothing has yet been described for a similar organization of area 24c in ACC. The M_2 receptors provide new information about the heterogeneity of area 24c, which can be subdivided into two parts: 24cv and 24cd. The laminar pattern of M_2 receptors in 24cv is similar to that described for 24b, but with a less pronounced minimum in layer III. Muscarinic M_2 receptor densities are not only lower in 24cd than in 24cv, but also more homogeneously distributed, with only a discrete maximum in layer V (Fig. 2.3).

Anterior midcingulate areas a24a´-b´, 24c´v, 24c´d, and 32´ contain higher mean M_2 receptor densities than areas 24a-b, 24cv, 24cd, and 32, respectively (Table 2.3). Area a24a´ presents a bilaminar pattern, with a local minimum in layer III (Fig. 2.4), which was not present in area 24a (Fig. 2.3). Conversely, the local minimum seen in layer III of areas 24b and 24cv (Fig. 2.3) is not present in areas a24b´ or 24c´v (Fig. 2.4). Area 24c´d shows a local maximum in layer V (Fig. 2.4), which is more prominent than that seen in area 24cd (Fig. 2.3). Area 32´ contains a higher mean M_2 receptor density than area 32 (Table 2.3), but presents the same laminar pattern (Figs. 2.3 and 2.4). Thus, the laminar pattern of the M_2 receptors in a24b´, 24c´v, and 24c´d is characterized by low concentrations in the superficial layers and high values in layer V. It is most important to realize, that M_2 regulation of aMCC occurs at the level of layer V. Layer Vb in this region contains corticospinal projection neurons. Thus, M_2 receptors are in a unique position to enhance layer V outflow to the spinal cord.

The laminar pattern of the M_2 receptors is drastically different in areas of pMCC. Areas p24a´ and p24b´ are characterized by clearly higher M_2 receptor densities in the superficial than in the deep layers (Fig. 2.5). Conversely, area 24dv presents low M_2 receptor densities in the superficial layers and a local maximum in layer V (Fig. 2.5). In area 24dd, M_2 receptors are homogeneously distributed throughout all cortical layers.

All divisions of posterior cingulate area 23 contain higher mean M_2 receptor densities than p24´ (Table 2.3). Areas 23d, d23, and v23 are characterized by clearly higher supragranular than infragranular M_2 receptor densities (Figs. 2.6–2.8), whereas area 23c presents a more homogeneous M_2 receptor distribution, with only slightly higher concentrations in the infragranular than in the supragranular layers (Fig. 2.7). Area 31 can be clearly distinguished from area 23 since it contains higher mean M_2 receptor densities and presents the opposite laminar pattern, with highest concentrations in the infragranular layers (Fig. 2.8).

The M_2 receptors are homogeneously distributed throughout retrosplenial area 29 (Fig. 2.7). Conversely, area 30 contains higher M_2 receptor densities in the supragranular than in the infragranular layers (Fig. 2.7). Area 29l contains slightly higher M_2 receptor densities than area 29m (Fig. 2.7). If it is true that the M_2 receptor is a presynaptic cholinergic autoreceptor, this suggests that areas 29 and 30 are differentially regulated by cholinergic afferents. In RSC, M_2 receptor actions would be the most important in regulating corticocortical actions in layer III.

Nicotinic receptors

The α4/β2 and α3 subtypes of nicotinic receptors were identified with the high affinity agonist [^{3}H]epibatidine (Perry and Kellar, 1995). In contrast to the muscarinic receptors, the nicotinic receptors present a rostrocaudal gradient in their mean areal densities. Lowest mean densities were measured in ACC and highest concentrations in PCC and RSC (Table 2.3). The laminar pattern of the nicotinic receptor differs significantly from that of the muscarinic receptors, and, as previously described for other brain regions (Zilles *et al.*, 2002a, 2002b, 2004), shows distinct variations within the cingulate cortex:

- Nicotinic receptors are homogeneously distributed throughout all cortical layers of some regions (e.g. 25),
- present two local maxima in other regions (e.g. 24a, a24a', p24a', 24b, a24b', p24b', 24cv, 24cd, 24c'c, 24c'd, 24dv, 24dd, 32, 32'),
- or a single maximum in layer IV in a third group of regions (e.g. 23d, 23c, d23, v23).

Anterior cingulate area 25 contains the lowest mean nicotinic receptor density measured within the cingulate cortex (Table 2.3). Furthermore, nicotinic receptors are homogeneously distributed throughout all layers of area 25 (Fig. 2.2). Since M_1 and M_2 receptors also have a relatively low expression in area 25, the only means by which cholinergic input can modulate area 25 function is through the M_3 receptor.

Areas 24a-c and 32 show a differential laminar pattern of the nicotinic receptors (Fig. 2.3). Area 24a has a maximum in layer I and slightly higher densities in layer III than in the adjacent layers. Area 24b has two clear maxima, of approximately the same intensity: the first in layer I and the second in layer IIIc. Furthermore, layer II and upper layer III contain lower nicotinic receptor densities than the infragranular layers. Area 24c also has maxima in layers I and IIIc. However, the former is more pronounced than the latter. The infragranular layers of 24c contain higher nicotinic densities than those of area 24b. Area 32 also contains two maxima; one located in layer I and the second one, flanked by two local minima, in layers IIIc-IV (Fig. 2.3).

Periallocortical area 33 contains slightly higher nicotinic receptor densities than area 24a, but comparable values to those measured in a24a´ and p24a´ (Table 3). However, nicotinic receptors are homogeneously distributed throughout all layers of area 33, thus enabling its delineation from all subdivisions of area 24 (Fig. 2.3).

The mean nicotinic receptor densities of anterior midcingulate areas a24a´-b´, 24c´, and 32´ are higher than those of areas 24a-c and 32, respectively (Table 2.3), but there are no considerable differences in the laminar patterns. Area a24a´ has a maximum in layer I and a second one, though less pronounced, in layer III (Fig. 2.4). Areas a24b´ and 24c´ have two clear maxima, of approximately the same intensity: the first in layer I and the second in layer IIIc (Fig. 2.4). However, layer V of a24b´ contains higher nicotine receptor densities than that of area 24b, whereas layer V of 24c´ contains lower nicotine receptor densities than that of 24c. Area 32´ also contains two maxima; one located in layer I and the second one in layers IIIc-IV (Fig. 2.4).

Posterior midcingulate areas p24a´-b´ and 24d contain slightly lower nicotinic concentrations than those measured in the rostrally adjacent regions (Table 3) as well as differing laminar patterns. Area p24a´ contains a first maximum in layer I and a second one, which is more pronounced, in layer III. Areas p24b´ and 24dv contain a first maximum in layer III followed by a second in layer Vb (Fig. 2.5). Area 24dd also presents maxima in layers III and Vb, although the latter one is less intense.

Areas of PCC contain higher nicotinic receptor densities than those measured in ACC or MCC (Table 2.3).

Additionally, the laminar pattern of the nicotinic receptors changes: all subdivisions of area 23 present a single maximum in layer III or IV, as well as slightly higher concentrations in the supragranular than in the infragranular layers (Figs. 2.6–2.8). In areas 23d and d23, the maximum is located in lower layer III, whereas in areas 23c and v23 it is found in layer IV. Area 31 contains higher nicotinic receptor densities than areas d23 or v23. Furthermore, nicotinic receptors are homogeneously distributed throughout all layers of area 31.

Retrosplenial areas 29 and 30 contain higher nicotinic receptor densities than area 23 (Table 6). Additionally, areas 29 and 30 present a maximum concentration of nicotinic receptors in layer IV. This maximum is slightly higher in layer IV of area 29m (Fig. 2.7).

Noradrenergic System

Noradrenergic function is fundamental to coordinating the actions of limbic structures. These include the ACC, amygdala, anterior insula, and orbitofrontal cortex, as well as subcortical emotional motor structures including the periaqueductal gray and the paraventricular nucleus of hypothalamus. Although the noradrenergic innervation of these structures is reviewed in detail in Chapter 22, α_1 adrenoceptors are presynaptic on noradrenergic terminals and provide a direct marker of such innervation. In contrast, the α_2 receptors are postsynaptic on cortical neurons. Both receptor subtypes have been identified based on their pharmacological profiles.

The α_1 receptor is the prevailing α-noradrenaline receptor subtype in the cingulate cortex. The α_1 and α_2 present different, receptor specific laminar patterns within the cingulate cortex. Both receptor subtypes are characterized by higher densities in the supragranular layers than in the infragranular ones. Additionally, α_2 receptors present a local maximum in layer I and a second slightly lower one in layer III. Neither of these receptor types presents a rostrocaudal gradient in their mean densities along the axis of the cingulate cortex. However, α_1 receptors present a dorsoventral gradient within area 24, with highest concentrations located within the callosal sulcus.

α_1 receptors

The α_1 receptors were labelled with the antagonist [^{3}H]prazosin. Their laminar pattern is characterized by higher densities in the supragranular layers than in the infragranular ones. Areas located in the posterior portion of the cingulate cortex present a local minimum in lower layer III and layer IV. This pattern is similar to that described for other regions of the human cerebral cortex (Zilles *et al.*, 2002b; Scheperjans *et al.*, 2005).

Anterior cingulate area 25 has highest α_1 receptor densities in layers I-II and lowest values in layer VI (Fig. 2.2). Areas 24a-c present highest densities in layers I-III followed by gradually decreasing concentrations, and lowest values are reached in layer VI (Fig. 2.3). Additionally, α_1 receptors present a dorsoventral gradient within area 24. Mean α_1 receptor densities are highest in area 24a and diminish through areas 24b and 24cv, reaching lowest values in 24cd. Area 32 contains lower α_1 receptor densities than area 24cd and a differing laminar pattern, since it presents highest densities in layers I-II, a minimum in layer III, and slightly higher values in the deep layers (Fig. 2.3). Periallocortical area 33 contains lower α_1 receptor densities than area 24a.

Anterior midcingulate areas a24a′-b′, 24c′, and 32′ contain lower mean α_1 receptor densities than those in areas 24a-c and 32 (Table 2.4). The dorsoventral

TABLE 2.4 Distribution of α-Noradrenaline Receptors Throughout Cingulate Cortex

Area	α_1	α_2
29l	218 ± 11	121 ± 1
29m	226 ± 47	126 ± 12
30	228 ± 45	124 ± 18
33	306 ± 51	87 ± 21
25	303 ± 45	129 ± 3
24a	369 ± 13	171 ± 37
a24a′	347 ± 52	94 ± 22
p24a′	312 ± 10	109 ± 14
24b	360 ± 11	167 ± 3
a24b′	325 ± 23	110 ± 23
p24b′	315 ± 20	125 ± 16
24cv	318 ± 1	171 ± 29
24cd	277 ± 1	168 ± 13
24c′v	256 ± 3	113 ± 29
24c′d	225 ± 11	125 ± 21
24dv	274 ± 65	129 ± 3
24dd	246 ± 20	125 ± 23
32	253 ± 11	143 ± 10
32′	232 ± 4	140 ± 12
23d	316 ± 73	148 ± 19
23c	310 ± 4	165 ± 22
d23	296 ± 26	142 ± 11
v23	263 ± 7	129 ± 32
31	316 ± 58	162 ± 1

Mean densities (±SD) in fmol/mg protein of the noradrenaline α_1 and α_2 receptors, which were labelled with [^{3}H]prazosin and [^{3}H]RX821002, respectively.

concentration gradient in area 24 is associated with highest densities in a24a′ and lowest values in 24c′d. Areas a24a′ and a24b′ can be distinguished due to the slightly higher concentration of α_1 receptors in the deep layers of the former region (Fig. 2.4). The deep layers of 24c′ contain higher α_1 receptor densities than those of a24b′ or 32′. Finally, the α_1 receptors are heterogeneously distributed throughout area 24c′: deep layers on the ventral bank of the cingulate sulcus contain clearly higher α_1 receptor densities than on the dorsal bank (Fig. 2.4). This confirms once again the neurochemical differentiation of area 24c on the ventral and dorsal banks of the cingulate sulcus.

There is no dorsoventral concentration gradient in α_1 receptor densities in pMCC (Table 2.4). This is because p24a′ and p24b′ contain comparable mean α_1 receptor densities. The laminar pattern of α_1 receptors in 24dv resembles that of area 32 (Fig. 2.3), with highest densities in layers I-II, a minimum in layers III and IV, and slightly higher values in the infragranular layers (Fig. 2.5). Area 24dd contains considerably fewer α_1 receptors in the infragranular layers.

Posterior cingulate areas 23d and 23c contain comparable concentrations of α_1 receptors, which are slightly higher than those measured in area d23 (Table 2.4). In turn, area d23 contains a higher mean α_1 receptor density than area v23. Additionally, all subdivisions of area 23 are characterized by higher concentrations in layers I-III than in layers V-VI and by a local minimum in layers III-IV (Figs. 2.6-2.8). This laminar pattern also applies to area 31, which contains a mean α_1 receptor density comparable to that of areas 23d and 23c.

Retrosplenial areas 29 and 30 contain lowest α_1 receptor densities of the cingulate cortex. They can be distinguished due to the higher α_1 receptor densities in the superficial layers of the latter area (Fig. 2.7). However, α_1 receptors do not enable the definition of the border between the medial and lateral components area 29 (Fig. 2.7).

In the framework of the presynaptic autoreceptor localization, there appears to be a mismatch in the localization of noradrenergic terminals, as described in Chapter 22, and the laminar distribution of α_1 receptors observed in this study. One explanation could be species differences, since data in Chapter 22 was acquired in monkey tissue and the present observations were made in human tissue. However, α_1 laminar distribution patterns are the same in human (present data) and monkey (Bozkurt *et al.*, 2005) cingulate cortices. Thus, the difference is likely due to the fact that dopamine-β-hydroxylase immunohistochemistry labels the entire axon tree and imparts a homogeneous appearance, while the [^{3}H]prazosin binding (labelling α_1 receptors) is selective for axon terminals and more likely approximates the distribution of the terminal axonal field.

α_2 receptors

The α_2 receptors were labelled with the selective antagonist [^{3}H]RX 821002. They do not present a rostrocaudal gradient in their mean densities along the axis of the cingulate cortex. The laminar pattern of the α_2 receptors remains constant in the isocortical cingulate regions: the supragranular layers contain clearly higher receptor densities than the infragranular ones. Additionally, a local maximum is present in layer I and a second slightly lower one, in layer III. This laminar pattern is comparable do that of the extrastriate visual cortex (Zilles *et al.*, 2002a).

Anterior cingulate area 25 contains a lower mean α_2 receptor density than areas 24a-c (Table 2.4). Furthermore, the superficial local maximum in area 25 is more pronounced than that of areas 24a-c (Fig. 2.2). Area 24b contains a lower α_2 receptor density than areas 24a or 24c (Fig. 2.3). Areas 32 and 24cd can be distinguished due to the lower concentration of α_2 receptors in the former area. Periallocortical area 33 contains lower α_2 receptor densities than area 24a (Table 2.4) and does not present the local minimum in layer II.

Mean α_2 receptor densities are lower in aMCC than in ACC (Table 2.4). However, they are comparable to the values measured in pMCC. Mean α_2 receptor densities increase gradually when moving from a24a′ to 24c′d and from p24a′ to 24dv. This is the opposite situation to that described at this level for the α_1 receptor densities. Area 24dd contains slightly lower α_2 receptor densities in the deep layers than area 24dv (Fig. 2.5). Furthermore, α_2 receptors also enable the subdivision of area 24c′ into a ventral (24c′v, abuts area a24b′) and a dorsal (24c′d, abuts area 32′) component (Fig. 2.4). Area 24c′v contains lower α_2 receptor densities than area 24c′d, particularly in the deep layers. The border between areas 24c′d and 32′ is visualized by an increase in the supragranular α_2 receptor densities in the latter area (Fig. 2.4).

Higher mean α_2 receptor densities were measured in posterior cingulate areas 23d and 23c than in areas d23 and v23, which in turn contain higher concentrations than those found in the most caudal subdivisions of area 24 (Table 2.4). Areas 23d and 23c can be distinguished based on the higher α_2 receptor density in the supragranular layers of the latter area (Fig. 2.7). Area 31 contains a clearly higher mean α_2 receptor density than d23 or v23, but comparable values to those found in 23c.

Retrosplenial areas 29 and 30 contain lower α_2 receptor densities than the adjacent isocortical areas (Table 2.4) as well as a simpler laminar pattern, since

these areas do not present the local minimum in layer II which is seen in the isocortical areas. Areas 29l and 29m cannot be delineated based on the distribution of α_2 receptors (Fig. 2.7).

In the framework of the presynaptic autoreceptor localization, there is a mismatch in the localization of noradrenergic innervation based on α_1 receptor binding and postsynaptic receptors. Since supragranular layers contain higher α_2 receptor densities than the infragranular ones, noradrenergic innervation enhances α_2 activation in superficial layers, while likely innervating a β receptor population in the infragranular layers (Vogt *et al.*, 1991).

Serotoninergic System

Serotonin receptors have been classified into seven families comprising a total of fourteen structurally, functionally, and pharmacologically different subtypes (for a review see Hoyer *et al.*, 2002). We examined the distribution of the 5-HT$_{1A}$ and the 5-HT$_2$ subtypes in the present study. The 5-HT$_{1A}$ receptor is the prevailing serotonin receptor subtype in ACC, whereas the 5-HT$_2$ receptor dominates in PCC. Additionally, 5-HT$_{1A}$ and 5-HT$_2$ receptors differ considerably in their laminar patterns, since the 5-HT$_{1A}$ receptors are characterized by high concentrations in the supragranular layers, whereas the opposite holds true for the 5-HT$_2$ receptors. The balance between both serotonin receptor subtypes not only changes between ACC and PCC, but also differs at a laminar level, with a major 5-HT$_{1A}$-mediated influence in layers I-II, and a dominating 5-HT$_2$-mediated influence in layers III-VI.

5-HT$_{1A}$ receptors

5-HT$_{1A}$ receptors were labelled with the selective agonist [^{3}H]8-OH-DPAT. They present a striking laminar pattern, which remains constant throughout all areas of the cingulate cortex, and is comparable to that described for PCC (Vogt *et al.*, 1990) and other cortical regions (Pazos *et al.*, 1987a; Hall *et al.*, 1997; Zilles *et al.*, 2002b, 2004): high densities in layers I-II are followed by low values in layers III-IV and a second maximum (though much lower than the superficial one) in layers V-VI.

Isocortical cingulate areas (i.e., everything but periallocortical areas 33, 29, and 30) contain clearly higher mean 5-HT$_{1A}$ receptor densities than the periallocortical ones (Table 2.5). However, within the isocortical portion of the cingulate cortex, most areas presented comparable mean 5-HT$_{1A}$ receptor densities, as well as a constant laminar pattern of this receptor subtype. Thus, most borders within the cingulate cortex are not visualized by the 5-HT$_{1A}$ receptors. However, it is once again interesting to note that the ventral and dorsal banks of the cingulate sulcus differ in their neurochemical structure. Areas 24cv and 24c´v contain higher receptor densities, particularly in the deep layers, than their dorsal counterparts.

From a clinical pathological perspective, area 25 presents one of the most interesting patterns of 5-HT$_{1A}$ binding. Since this region is particularly vulnerable in depression, as discussed below and in Chapter 25, the selective actions of antidepressant drugs might be determined by the 5-HT$_{1A}$ receptor content of this area. Thus, area 25 has the highest density of 5-HT$_{1A}$ receptors in the cingulate gyrus (Table 2.5). Superficial layers contain significantly higher 5-HT$_{1A}$ receptor densities than deeper layers (Fig. 2.2).

5-HT$_2$ receptors

The 5-HT$_2$ receptors were labelled with the antagonist [^{3}H]ketanserin. They are in higher concentrations in PCC than in ACC (Table 2.5). The laminar pattern of the

TABLE 2.5 Densities of Serotonin Receptors Throughout Cingulate Cortex:

Area	5-HT$_{1A}$	5-HT$_2$
29l	196 ± 59	331 ± 21
29m	228 ± 104	330 ± 3
30	222 ± 96	305 ± 34
33	417 ± 49	210 ± 74
25	523 ± 83	288 ± 6
24a	451 ± 73	282 ± 85
a24a´	387 ± 46	213 ± 70
p24a´	358 ± 23	205 ± 7
24b	348 ± 33	260 ± 10
a24b´	340 ± 18	179 ± 37
p24b´	370 ± 1	220 ± 5
24cv	356 ± 30	224 ± 10
24cd	337 ± 29	221 ± 6
24c´v	276 ± 28	183 ± 57
24c´d	264 ± 1	178 ± 51
24dv	354 ± 109	200 ± 5
24dd	308 ± 74	178 ± 2
32	335 ± 27	228 ± 20
32´	162 ± 51	273 ± 72
23d	352 ± 123	310 ± 19
23c	399 ± 90	279 ± 11
d23	259 ± 72	300 ± 53
v23	216 ± 56	233 ± 60
31	342 ± 44	284 ± 3

Mean densities (±SD) in fmol/mg protein of the serotonin 5-HT$_{1A}$ and 5-HT$_2$ receptors, which were labelled with [^{3}H]8-OH-DPAT and [^{3}H]ketanserin, respectively.

5-HT_2 receptors is characterized by high densities in layers III-V, intermediate concentrations in layers I-II, and low values in layer VI. This pattern is in agreement with previous autoradiographical reports of 5-HT_2 receptor distribution (Pazos *et al*., 1987b; Vogt *et al*., 1990; Zilles *et al*., 2002a, 2004) as well as with the observations made from *in situ* hybridisation studies (Burnet *et al*., 1995; Pasqualetti *et al*., 1996).

Anterior cingulate areas 25, 24a, and 24b contain comparable mean 5-HT_2 receptor densities, which are higher than those measured in areas 24c or 32 (Table 2.5). 5-HT_2 receptors do not show the border between 24dv and 24dd (Fig. 2.3). Area 32 contains higher 5-HT_2 receptor densities, particularly in the supragranular layers than area 24cd. Periallocortical area 33 contains relatively low 5-HT_2 receptor densities.

Anterior midcingulate areas a24a´-b´, 24c´v, and 24c´d contain lower mean 5-HT_2 receptor densities than the rostrally adjacent areas. Conversely, higher concentrations of 5-HT_2 receptor were measured in area 32´ than in area 32. Areas a24b´, 24c´v, and 24c´d do not differ in their mean 5-HT_2 receptor densities, which are lower than those measured in a24a´ (Table 2.5).

Mean 5-HT_2 receptor concentrations of posterior midcingulate areas p24a´-b´, 24dv, and 24dd are slightly higher than those of the rostrally adjacent areas. Area p24b´ contains a higher mean 5-HT_2 receptor density than p24a´ or 24dv. Area 24dd contains lower 5-HT_2 receptor densities than 24dv (Fig. 2.5).

Mean 5-HT_2 receptor densities are considerably higher in posterior cingulate areas 23 and 31 than in pMCC (Table 2.5). Areas 23c, d23, and 31 contain comparable mean 5-HT_2 receptor concentrations, which are lower than those of area 23d, but higher than those measured in area v23.

Retrosplenial areas 29 and 30 contain the highest mean concentrations measured in the cingulate cortex (Table 2.5). Area 29 contains higher 5-HT_2 receptor densities than area 30 (Fig. 2.7). However, the 5-HT_2 receptors do not show the lateral and medial subdivisions of area 29 (Fig. 2.7).

Dopaminergic System

Dopamine acts via two receptor families ($D_{1\text{-like}}$ and $D_{2\text{-like}}$) to provide an essential modulation of glutamatergic and GABAergic neurotransmission during the regulation of motor, affective and cognitive functions (Cowan *et al*., 1994; Sesack *et al*., 1995). Binding of dopamine to D_1 receptors results in a neuronal activation, which is countered by the simultaneous inhibitory actions of D_2 receptors as discussed in detail in Chapter 7.

Alterations in the dopaminergic systems are thought to be crucial in the aetiology of schizophrenia, since high doses or chronic administration of amphetamine (resulting in an increased dopamine release) induce a psychosis which is indistinguishable from acute paranoid schizophrenia (Randrup and Munkvad, 1965), whereas antipsychotic drugs block dopamine receptors (Seeman *et al*., 1976). However, studies carried out during the last three decades have not only failed to provide conclusive evidence to support a general hyperactivity of dopaminergic neurons in schizophrenia, but have also implicated other neurotransmitters such as glutamate and serotonin (for reviews see Reynolds, 1995; Glenthøj and Hemmingsen, 1999). Functional imaging studies have demonstrated a marked disruption of dopamine function in drug-addicted subjects, which is associated with reduced activity of the orbitofrontal cortex and ACC. However, these hypoactive regions become hyperactive when addicted subjects are exposed to drug-related stimuli as well as during the drug-craving period (Adinoff, 2004; Volkow *et al*., 2004). Moreover, the compulsive drive toward drug use is complemented by deficits in impulse control and decision making, which are also mediated by ACC and the orbitofrontal cortex (Adinoff, 2004; Volkow *et al*., 2004).

The specific involvement of ACC in processes modulated by the dopaminergic system is not surprising, since it is the cortical region with the most dense dopaminergic innervation (Thierry *et al*., 1973; Conde *et al*., 1995a), dopaminergic neurons have been shown to use glutamate as a co-transmitter (Trudeau, 2004), and D_1 receptors also modulate glutamatergic signalling via an increased externalization of AMPA receptors (Wolf *et al*., 2003). Additionally, ACC contains higher mean densities of glutamate AMPA and kainate and dopamine D_1 receptors than PCC (Tables 2.1 and 2.6).

D_1 receptors

In the present study D_1 receptors were labelled with the antagonist [^{3}H]SCH 23390 (Billard *et al* 1984). Within area 24, D_1 receptors present a rostrocaudal gradient in their mean areal densities, with lowest concentrations located in the posterior subdivisions of this region (Table 2.6). Posterior cingulate areas 23 and 31 contain higher D_1 receptor densities than MCC, but lower values than ACC (Table 2.6). Binding sites of the D_1 receptor are concentrated largely in the superficial layers I-III. This laminar pattern coincides with that described previously for the primary motor cortex based both on autoradiographical (Lidow *et al*. 1990; Zilles *et al*. 2002b) and on immunohistochemical studies (Smiley *et al*. 1994).

Anterior cingulate area 24a contains the highest concentration of D_1 receptors measured in the cingulate cortex (Table 2.6). Although area 24b shows lower D_1 receptor densities in the deep layers than 24c, it contains higher concentrations in the superficial layers (Fig. 2.3), thus resulting in a comparable mean receptor

density for both areas (Table 2.6). Area 32 has an overall lower mean receptor density than area 24c (Table 2.6). Periallocortical area 33 contains high D_1 receptor densities.

Anterior midcingulate areas a24a′-b′, 24c′, and 32′ contain lower mean D_1 receptor densities than areas 24a-c and 32 (Table 2.6). Area a24a′ presents a higher concentration if D_1 receptors, particularly in the infragranular layers, than area a24b′ (Fig. 2.4). Area 24c′ has slightly lower D_1 receptor densities in layers III-VI than area a24b′ (Fig. 2.4) but overall higher densities than area 32′ (Fig. 2.4).

Mean D_1 receptor densities decrease further in posterior midcingulate areas p24a′-b′, 24dv, and 24dd (Table 2.6). Areas p24a′ and p24b′ contain comparable mean D_1 receptor concentrations, which are higher than those measured in areas 24dv and 24dd. The D_1 receptors do not show the subdivision of area 24d into its dorsal and ventral parts (Fig. 2.5).

Posterior cingulate areas 23d, 23c, d23, v23, and 31 contain considerably higher mean D_1 receptor densities than those measured in pMCC (Table 2.6). D_1 receptors do not show subdivisions of area 23, since areas 23d, 23c, d23, and 31 present comparable D_1 receptor concentrations, which are only slightly higher than those measured in area v23. Retrosplenial areas contain relatively high D_1 receptor densities (Table 2.6). The D_1 receptors do not differentiate the medial and lateral subdivision of area 29 (Fig. 2.7).

There appears to be a striking mismatch between midcingulate gyral and sulcal dopamine innervation as shown with tyrosine hydroxylase immunohistochemistry and [^{3}H]SCH23390 binding (D_1 receptors). This is a particularly important issue since reward mechanisms drive dopaminergic innervation to the rostral cingulate motor area in the cingulate sulcus. Interestingly, D_1 receptor densities are higher in the gyral areas than in the sulcal ones, particularly for the supragranular layers. Although dopamine innervation of the gyral surface is considerably lower than that of the sulcus, the opposite distribution of the D_1 receptor may compensate for this difference. Thus, the D1 state hypothesized by Seamans and Yang (2004) and discussed in detail in Chapter 7, may equally engage both portions of the cingulate cortex.

TABLE 2.6 Densities of D_1 Receptors Throughout Cingulate Cortex

Area	D_1
29l	62 ± 2
29m	60 ± 3
30	60 ± 1
33	73 ± 15
25	81 ± 5
24a	95 ± 20
a24a′	71 ± 14
p24a′	45 ± 1
24b	77 ± 9
a24b′	62 ± 7
p24b′	43 ± 5
24cv	73 ± 1
24cd	74 ± 7
24c′v	53 ± 5
24c′d	53 ± 5
24dv	40 ± 7
24dd	35 ± 2
32	53 ± 5
32′	48 ± 7
23d	68 ± 3
23c	65 ± 8
d23	65 ± 2
v23	57 ± 10
31	68 ± 2

Mean densities (±SD) in fmol/mg protein of the dopamine D_1 receptors, which were labelled with [^{3}H]SCH23390.

Cingulate Regional Neurotransmitter Organization

Receptor fingerprint analysis

Receptor fingerprints are polar coordinate plots in which the areal densities (receptor densities averaged over all cortical layers and brains) of various receptors quantified in one architecturally defined area are visualized simultaneously (Fig. 2.9). The shape and size of the fingerprint are outlined by the lines connecting the areal densities. Receptor fingerprints demonstrate the balance between different receptor types and transmitter systems within a single area (Zilles and Palomero-Gallagher, 2001; Zilles *et al.*, 2002a, 2002b). The shape and size of a fingerprint are specific for each area, and differences in shape and/or size are found between cortical areas of different functions and architecture (Zilles and Palomero-Gallagher, 2001; Zilles *et al.*, 2002a; Palomero-Gallagher and Zilles, 2004). Furthermore, the degree of dissimilarity in shape and/or size between areal specific fingerprints seems to reflect the degree of dissimilarity both in architecture and function of the areas in question (Zilles *et al.*, 2002a). Additionally, variations in the size but not in shape of fingerprints may represent different hierarchical levels within a functional system, since fingerprints of macaque primary mesial motor areas were shown (Geyer *et al.*, 1998)

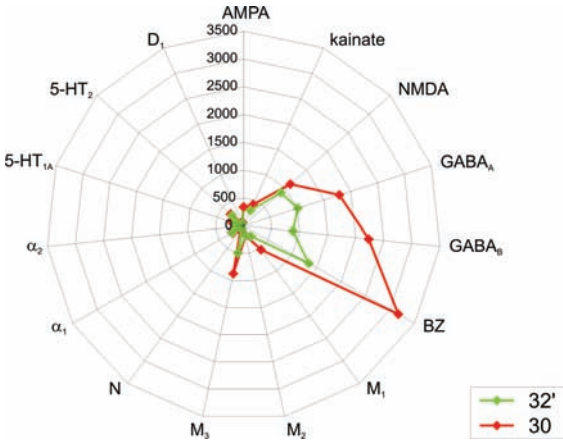

Fig. 2.9 Two extreme cingulate receptor fingerprints. Mean densities of AMPA, kainate, NMDA, $GABA_A$, $GABA_B$, BZ, M_1, M_2, M_3, nicotinic (N), α_1, α_2, 5-HT_{1A}, 5-HT_2, and D_1 binding sites are displayed in a polar coordinate plot (binding site densities in 0-3500 fmol/mg protein). The lines connecting the mean densities (shown with romboids) of the receptor types measured in each cytoarchitecturally identified cortical area define the contour of the fingerprint, which demonstrates the balance between different receptor types and transmitter systems within a single area. The shapes and sizes of the fingerprints are specific for each area. Differences in size indicate variations in absolute receptor densities, but the balance between receptor types is the same in all regions. Conversely, differences in shape indicate variations in the balance between receptor types. Differences in receptor fingerprints reveal aspects of the brain's hierarchical organization.

to be identical in shape (all three areas are involved in "motor" functions), but differ in size (i.e., proportionally increasing receptor densities from the primary motor to the supplementary to the pre-supplementary motor areas).

Receptor fingerprints of the cingulate areas differ in both their shapes and sizes (Figs. 2.9–2.12). Areas of ACC (Fig. 2.10) and MCC (Fig. 2.11) are characterized by relatively small receptor fingerprints, thus reflecting the fact that they contain lower receptor densities than areas located in PCC (Fig. 2.12) and RSC (Fig. 2.12). The functional implications of differences in the shape and size of receptor fingerprints are discussed in detail in the following section.

Multivariate Models

Working on the hypothesis that transmitter receptors reveal neurochemically coherent groups of areas as implicated by the four-region neurobiological model, we carried out descriptive statistical tests such as a multidimensional scaling and a K-means clustering procedure in order to determine the clustering of cingulate regions according to their neurochemical structure. All statistical procedures were performed using Matlab Statistics Toolbox (MatLab 7.1; Mathworks Inc., Natick, MA, USA).

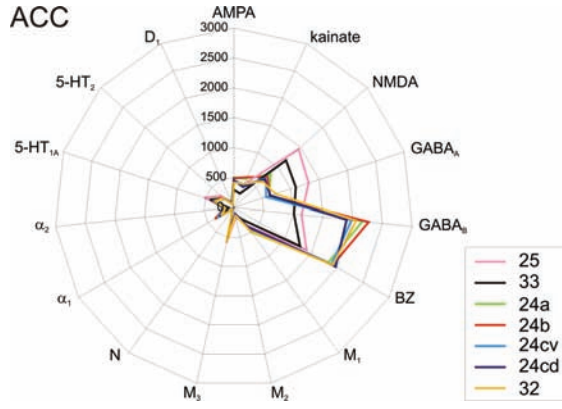

Fig. 2.10 Receptor fingerprints of anterior cingulate cortical areas.

The multidimensional scaling test enables the representation in a small number of dimensions (two in this application), of distances between the *n*-dimensional feature vectors. We used the goodness-of-fit criterion "stress" to optimize the non-linear approximation of the interareal distances in the two-dimensional configuration shown in Figure 2.13 with respect to the original, 15-dimensional feature space (one feature for

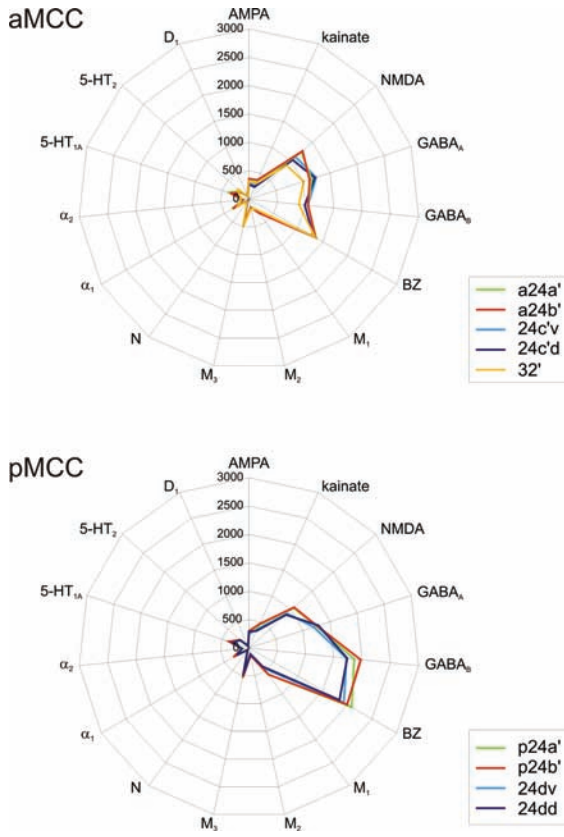

Fig. 2.11 Receptor fingerprints of midcingulate cortical areas.

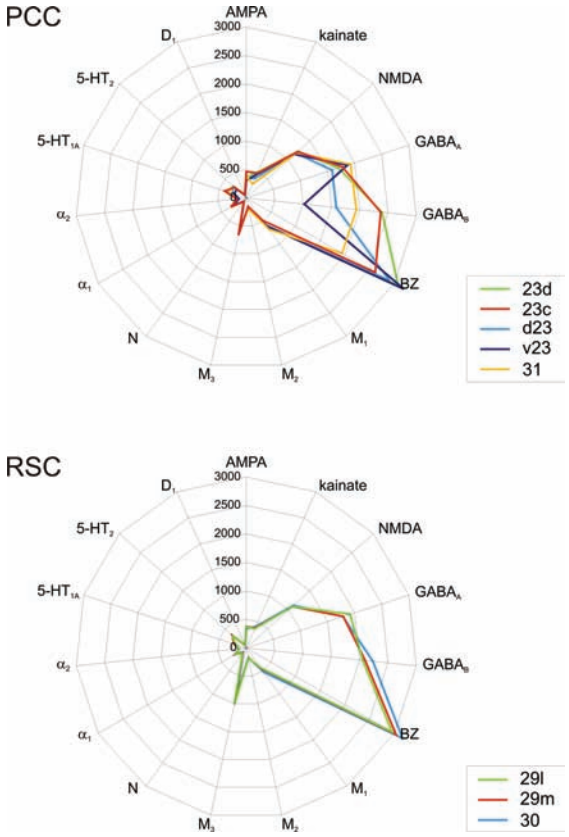

Fig. 2.12 Receptor fingerprints of posterior cingulate and retrosplenial cortices.

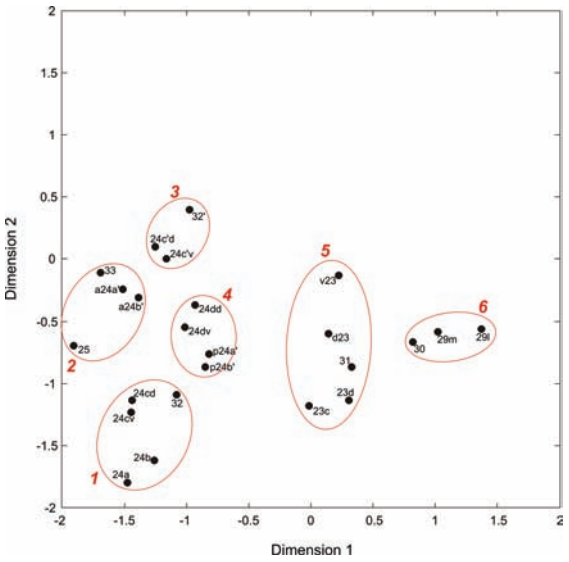

Fig. 2.13 Multidimensional scaling plot resulting from the analysis of the areal densities of glutamate (AMPA, kainate, NMDA), GABA (GABA$_A$, GABA$_B$, BZ), acetylcholine (muscarinic M$_1$, M$_2$, M$_3$, nicotinic), noradrenaline (α_1, α_2), serotonin (5-HT$_{1A}$, 5-HT$_2$), and dopamine (D$_1$) receptors in the cingulate areas. The information in a fingerprint is treated as a feature vector with 15 elements, each of which represents the areal density of a distinct transmitter receptor in that area. "Dimension 1" and "Dimension 2" are axes in the two-dimensional representation of the 15-dimensional feature space. Each labelled point represents the position of a cingulate area. The labelled ellipses were added to demonstrate the coincidence of the areal clusters with the result of the K-means clustering.

each of the examined receptor types). The low stress value (0.1063) indicates a good approximation. Within a given area, absolute densities differed considerably between the different receptor types (e.g. 62 fmol/mg protein D$_1$ receptors versus 2955 fmol/mg protein BZ binding sites in the lateral part of area 29). Therefore, the total binding values were normalized by dividing each areal density by the overall receptor density of that receptor (average of the densities of this receptor across all areas investigated) prior to calculating Euclidean distances between areas as a measure of dissimilarity between fingerprints.

To determine the number of natural clusters, we applied a K-means clustering. Each cluster in the partition is defined by its member areas and by its centroid, that is, the point to which the sum of distances from all areas in that cluster is minimized. Working on the basis of a predefined number of clusters (K), areas are iteratively shuffled between clusters until the smallest sum of distances from each area to its cluster centroid is reached. The result is a set of clusters that are as compact and well separated as possible. The average silhouette value (mean[silh$_K$]) is a parameter indicating the degree of separation between clusters and thus indicates the meaningfulness of the predetermined number of clusters. The results for four runs (K = 5, 6, 7) indicate that the six cluster solution is the most meaningful, since this partition resulted in the average silhouette value closest to 1 (mean[silh$_5$] = 0.5838, mean[silh$_6$] = 0.5885, mean[silh$_7$] = 0.5882).

Additionally, in a recent study we examined the grouping of cingulate areas according to the degree of similarity of their receptor fingerprints as determined by a hierarchical clustering analysis (Palomero-Gallagher *et al.*, 2008). As visualized in Figure 2.14, we could demonstrate that receptor binding sites segregate ACC and MCC from PCC and RSC, since ACC/MCC contain lower GABA$_A$, nicotinic and BZ, but higher 5-HT$_{1A}$ binding site densities than PCC/RSC. Interestingly, area 25 does not cluster with the remaining areas of ACC, but is associated with areas of MCC. The separation of area 25 from the neighboring pACC and clustering with the aMCC was found to be dependent on the densities of NMDA, GABA$_A$ GABA$_B$, and 5-HT$_{1A}$ receptors highlights a more complex functional organization of this area (Palomero-Gallagher *et al.*, 2008).

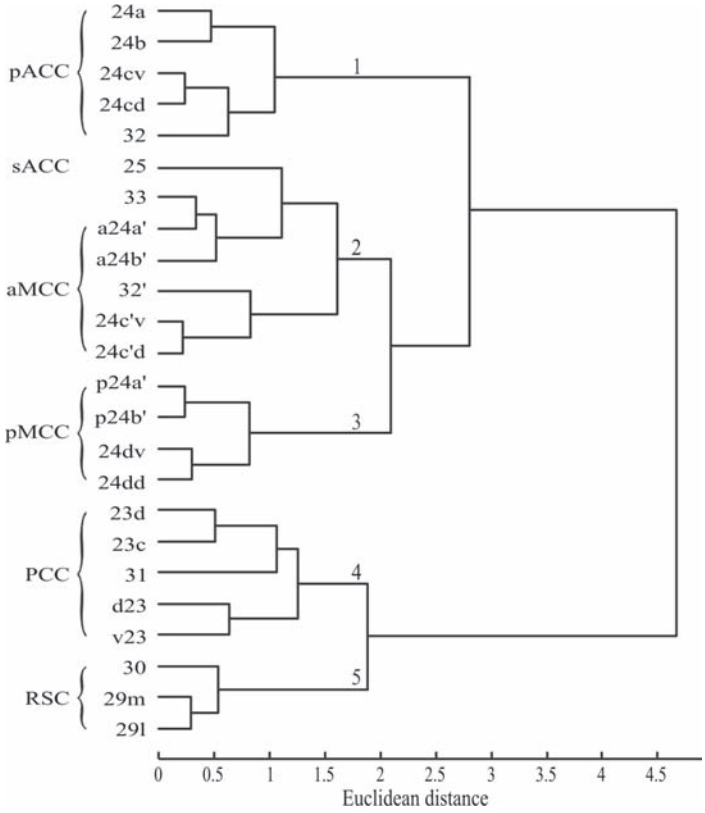

Fig. 2.14 Hierarchical clustering resulting from the analysis of the areal densities of glutamate (AMPA, kainate, NMDA), GABA ($GABA_A$, $GABA_B$, BZ binding), acetylcholine (muscarinic M_1, M_2, M_3, nicotinic), noradrenaline (α_1, α_2), serotonin (5-HT_{1A}, 5-HT_2), and dopamine (D_1) receptors in the cingulate areas.

Additionally, receptor binding sites segregate the anterior and posterior components of MCC. The pMCC contains higher $GABA_B$ and BZ but lower AMPA, M_2, and D_1 binding site densities than aMCC. PCC and RSC differ from each other by the higher M_1 and α_1 but lower M_3 binding site densities in PCC compared with RSC.

Therefore, the cluster analysis of the neurochemical structure of the human cingulate cortex enables its parcellation into ACC, MCC, PCC, and RSC, therefore further supporting the four-region neurobiological model of the cingulate gyrus. Moreover, MCC is more similar from the neurochemical point of view to ACC than to PCC, thus reflecting their closer functional relationship since PCC is involved in evaluative processes, whereas ACC and MCC are involved in the affective and cognitive aspects of executive processes, respectively, as discussed in Chapter 1.

Clinical Implications of Transmitter System Organization

Glutamatergic neurotoxicity in neurodegenerative disorders

Glutamate-mediated excitotoxicity is thought to contribute to cell injury and death in numerous neurodegenerative disorders such as Alzheimer's and Parkinson's diseases. It occurs via activation of glutamate receptors, in particular of the NMDA subtype (Frandsen and Schousboe, 2003; Arundine and Tymianski, 2004; Molinuevo *et al.*, 2005; Wenk, 2006; Chen and Lipton, 2006; Kwak and Weiss, 2006; Cull-Candy *et al.*, 2006). Overactivation of NMDA receptors results in excessive Ca^{2+} influx through the receptor's associated ion channel, which initiates a cascade of events including enzymatic processes and the release of damaging free radicals finally resulting in cell death.

Glutamate plays a key role in the neural processes underlying learning and memory, and it has been hypothesized that a disruption of glutamatergic function underlies the cognitive deficits seen in patients with Alzheimer's disease and other dementias (Danysz *et al.*, 2000; Molinuevo *et al.*, 2005). The continuous activation of NMDA receptors in these patients not only leads to the neurodegenerative processes just described, but also impairs long-term potentiation and synaptic plasticity, that is, learning (Danysz *et al.*, 2000).

The posterior cingulate cortex is the cingulate region most vulnerable to Alzheimer's disease (Johnson *et al.*, 2005) and is already affected in patients with a mild cognitive impairment which later progressed to

Alzheimer's disease (Anchisi *et al.*, 2005). Interestingly, PCC is the cingulate region with the highest mean NMDA receptor densities. Thus, recent efforts have focused on treatment of the cognitive symptoms of Alzheimer's disease using NMDA receptor antagonists, that is, agents that block NMDA receptor stimulation by preventing the passage of Ca^{2+} through the associated calcium channels (Molinuevo *et al.*, 2005; Chen and Lipton, 2006).

Benzodiazepine binding site

The action of GABA is allosterically modulated by a wide variety of chemical entities which interact with distinct binding sites at the $GABA_A$ receptor complex. Each subunit of the $GABA_A$ receptor, a heteromeric pentamer, has four transmembrane domains as well as a large extracellular N-terminal region containing separate binding sites for GABA and for various modulators (Macdonald and Olsen, 1994). One of the most thoroughly investigated modulatory sites is the benzodiazepine binding site, which acts by enhancing the $GABA_A$ receptor function in the brain and thus induces sedative, hypnotic, anxiolytic, and anticonvulsant activities.

As discussed by Faymonville *et al.* in Chapter 17 of this volume, aMCC is particularly active during pain modulation under hypnosis and its activity is highly correlated with that in a number of other areas that are a part of the pain neuromatrix. To the extent that BZs have hypnotic properties, it might be expected that the aMCC has a particularly high level of binding. Although BZ binding is high in sACC and pACC, there is not a particularly high level in aMCC (Table 2.2). We conclude that the hypnotic effects of BZ compounds are either attributable to a region that is less hypnotically sensitive in the cingulate gyrus or this property is the result of other cortical or subcortical binding sites. Of course, the high level of BZ binding in the ACC may confirm these compounds with anxiolytic properties. A review of the receptor fingerprints confirms this general view about BZ binding and emphasizes that PCC also has a high level of binding which is even greater than that in ACC. The functional consequences of BZ binding in PCC is not known, however, these polar plots of the receptor binding fingerprints provides a number of interesting hypotheses.

Mood disorders: GABAergic, noradrenergic, and serotoninergic systems

Alterations of the noradrenergic and serotoninergic systems have long been postulated to play a crucial role in the pathophysiology and subsequent treatment of mood disorders. Recent evidence suggests that serotonergic involvement in depression may be modulated by the action of GABA (Matsumoto *et al.*, 2007), and altered GABAergic function is also evident in depressed patients and in animal models of depression (Bhagwagar *et al.*, 2007; Grønli *et al.*, 2007). Interestingly, highest serotonin 5-HT_{1A}, GABA, ($GABA_A$ and $GABA_B$ receptors, BZ binding sites) and noradrenaline α_1 and α_2 receptor densities were found in ACC, the cingulate region most frequently involved in mood disorders, as discussed in detail in Chapters 11, 22, 24, and 25.

Major depression and bipolar disorder would be directly related to a low or high activity of norepinephrine-containing neurons, respectively. Activation of the α_1 receptors has been reported to facilitate the release of glutamate in ACC (Marek and Aghajanian, 1999). Additionally, this norepinephrine-stimulated glutamate release is thought to act via AMPA receptors (Marek and Aghajanian, 1999). Since the α_1 receptors do not show a density gradient along the rostrocaudal axis of the cingulate cortex, but the AMPA receptors are present in higher concentrations in the rostral cingulate areas, this region-specific effect could be explained by the rostrocaudal differences in the mean densities of glutamate receptors. Likewise, since blockage of α_2 receptors results in elevated brain levels of glutamate, serotonin, or dopamine release (Hanson and Ronnback, 1992; Blier, 2001; Devoto *et al.*, 2001), the region-specific effect of anxiolytic and antidepressant drugs specifically targeting the α_2 receptor could be explained by the differential distribution of receptors for these neurotransmitters.

The serotoninergic system has been implicated in the aetiology of a wide range of pathological states, including depression, anxiety, social phobia, Alzheimer's disease, schizophrenia, and eating disorders (Coppen and Wood, 1982; Akhodzadeh, 2001; Carter *et al.*, 2001; Versijpt *et al.*, 2003; Neumeister *et al.*, 2004). Although it has long been known that drugs which increase serotoninergic activity generally exert antidepressant effects on patients, it has not yet been possible to directly correlate a serotonin deficiency with depression. However, the interaction of low serotonin levels with other neurotransmitter systems is considered to be important in the aetiology of depression (Meltzer and Lowy, 1987). Numerous studies have described structural and functional abnormalities of ACC in schizophrenia (Carter *et al.*, 2001; Heckers *et al.*, 2004). Early theories of schizophrenia implicated a disturbed serotonin neurotransmission (Gaddum and Hameed, 1954; Woolley and Shaw, 1954). However, it is currently assumed that altered serotonin-dopamine and/or serotonin-glutamate interactions could be of more importance than changes in the individual systems (Wadenberg *et al.*, 1996; Aghjanian and Marek, 2000).

Alterations of the serotoninergic system are also thought to play a crucial role in the pathophysiology of eating disorders (Kaye *et al.*, 2005). Patients suffering from anorexia nervosa presented significantly lower 5-HT_{2A} receptor densities in ACC than age-matched controls (Bailer *et al.*, 2004). Additionally, functional imaging studies have demonstrated that ACC of anorectics is hypoperfused during rest conditions (Takano *et al.*, 2001), but more intensely activated by food-related stimuli when compared to that of age-matched controls (Ellison *et al.*, 1998; Uher *et al.*, 2003; Uher *et al.*, 2004). Interestingly, ACC forms part of a functional network involved in the establishment of the "notion of the self" (Posner and Rothbart, 1998; Kjaer *et al.*, 2002), and abnormalities in perception and evaluation of body shape are a hallmark of eating disorders (Frank *et al.*, 2004; Uher *et al.*, 2005).

The ACC, and in particular its infragranular layers, is richly innervated by serotoninergic fibers ascending from the dorsal and medial Raphe nuclei (Lidov *et al.*, 1980) and it is also the cortical region with the most dense dopaminergic innervation (Thierry *et al.*, 1973; Conde *et al.*, 1995b). Furthermore, ACC not only presents higher 5-HT_{1A} receptor densities (Table 2.5) than PCC, but it also contains higher densities of receptors for glutamate and dopamine (Tables 2.1 and 2.6, respectively), two neurotransmitter systems with which serotonin is known to interact (Wadenberg *et al.*, 1996; Aghjanian and Marek, 2000). Taken together, these data further support the notion that ACC may be an important cortical site in the therapeutic actions of antidepressant and antipsychotic drugs which selectively target the serotoninergic system (Mayberg *et al.*, 1997; Smith *et al.*, 2002; Celada *et al.*, 2004; Milano *et al.*, 2004; Seedat *et al.*, 2004).

Increasing evidence suggests that abnormalities in GABA neurotransmission are associated with the neurobiology of mood disorders, although the molecular mechanisms that may cause or contribute to the dysregulation of the GABAergic system remain unknown. Studies examining the association between post-trauma plasma GABA levels and long-term post-traumatic stress disorder (PTSD) and major depressive disorder revealed that mean post-trauma GABA levels were significantly lower among subjects who met criteria for PTSD (two-thirds of these patients also met criteria for major depressive disorder) than among those who did not (Vaiva *et al.*, 2004; Vaiva *et al.*, 2006). Additionally, recurrent depression has been associated with decreased GABA levels in ACC (Bhagwagar *et al.*, 2007), and resting-state concentration of GABA in the healthy human ACC has been demonstrated to predict the strength of negative BOLD responses during emotional processing (Northoff *et al.*, 2007). Since sACC contained significantly higher $GABA_A$, $GABA_B$, and BZ binding densities than pACC and sACC has a role in storing negatively valenced epidoic memories, we speculate that this pattern of findings indicates a high level of GABAergic activity in sACC which could isolate memories of sad events and stop them from "over participting" in conscious processes, since one would assume that constant access to sad memories would produce an altered mood.

Acknowledgements

The authors express their sincere thanks to Angelika Börner, Markus Cremer, Nadine Dechering, Stephanie Krause, Manuela Labsch, and Sabine Wilms for excellent technical assistance. They are also deeply indebted to Axel Schleicher and Brent Vogt for numerous hours of fruitful discussions. This Human Brain Project/Neuroinformatics research was funded jointly by the National Institute of Mental Health, of Neurological Disorders and Stroke, of Drug Abuse, and the National Cancer Centre.

References

Adinoff, B. (2004). Neurobiologic processes in drug reward and addiction. *Harv Rev Psychiatry 12*: 305–320.

Aghjanian, G. K., Marek, G. J. (2000). Serotonin model of schizophrenia: emerging role of glutamate mechanisms. *Brain Res Rev 31*: 302–312.

Akhodzadeh, S. (2001). The 5-HT hypothesis of schizophrenia. *IDrugs 4*: 295–300.

Akiyama, G., Ikeda, H., Matsuzaki, S., Sato, M., Moribe, S., Koshikawa, N., Cools, A. R. (2004). $GABA_A$ and $GABA_B$ receptors in the nucleus accumbens shell differentially modulate dopamine and acetylcholine receptor-mediated turning behaviour. *Neuropharmacology 46*: 1082–1088.

Alcantara, A. A., Mrzljak, L., Jakab, R. L., Levey, A. I., Hersch, S. M., Goldman-Rakic, P. S. (2001). Muscarinic m1 and m2 receptor proteins in local circuit and projection neurons of the primate striatum: anatomical evidence for cholinergic modulation of glutamatergic prefronto-striatal pathways. *J Comp Neurol 434*: 445–460.

Anchisi, D., Borroni, B., Franceschi, M., Kerrouche, N., Kalbe, E., Beuthien-Beumann, B., Cappa, S., Lenz, O., Ludecke, S., Marcone, A., Mielke, R., Ortelli, P., Padovani, A., Pelati, O., Pupi, A., Scarpini, E., Weisenbach, S., Herholz, K., Salmon, E., Holthoff, V., Sorbi, S., Fazio, F., Perani, D. (2005). Heterogeneity of brain glucose metabolism in mild cognitive impairment and clinical progression to Alzheimer disease. *Arch Neurol 62*: 1728–1733.

Araujo, F., Tan, S., Ruano, D., Schoemaker, H., Benavides, J., Vitorica, J. (1996). Molecular and pharmacological characterization of native cortical γ-aminobutyric $acid_A$ receptors containing both α_1 and α_3 subunits. *J Biol Chem 271*: 27902–27911.

Arundine, M., Tymianski, M. (2004). Molecular mecahnisms of glutamate-dependent neurodegeneration in ischemia and traumatic brain injury. *Cell Mol Life Sci 61*: 657–668.

Atzori, M., Kanold, P., Pineda, J. C., Flores-Hernández, J. (2003). Dopamine-acetylcholine interactions in the modulation of glutamate release. *Ann NY Acad Sci 1003*: 346–348.

Bailer, U. F., Price, J. C., Meltzer, C. C., Mathis, C. A., Frank, G. K., Weissfeld, L., McConaha, C. W., Henry, S. E., Brooks-Achenbach, S., Barbarich, N. C., Kaye, W. H. (2004). Altered 5-HT_{2A} Receptor binding after recovery from bulimia-type anorexia nervosa: relationships to harm avoidance and drive for thinness. *Neuropsychopharmacology 29*: 1143–1155.

Bhagwagar, Z., Wylezinska, M., Jezzard, P., Evans, J., Boorman, E., Matthews, M., Cowen, J. (2007). Low GABA concentrations in occipital cortex and anterior cingulate cortex in medication-free, recovered depressed patients. *Int J Neuropsychopharmacol 1–6*.

Blier, P. (2001). Crosstalk between the norepinephrine and serotonin systems and its role in the antidepressant response. J *Psychiatry Neurosci 26*: S3–S10.

Bozkurt, A., Zilles, K., Schleicher, A., Kamper, L., Sanz Arigita, E., Uylings, H. B., Kötter, R. (2005). Distributions of transmitter receptors in the macaque cingulate cortex. *Neuroimage 25*: 219–229.

Burnet, P. W. J., Eastwood, S. L., Lacey, K., Harrison, P. J. (1995). The distribution of 5-HT_{1A} and 5-HT_{2A} receptor mRNA in human brain. *Brain Res 676*: 157–168.

Carter, C. S., MacDonald, III A. W., Ross, L. L., Stenger, V. A. (2001). Anterior cingulate cortex activity and impaired self-monitoring of performance in patients with schizophrenia: an event-related fMRI study. *Am J Psychiatry 158*: 1423–1428.

Celada, P., Puig, M. V., Amargós-Bosch, M., Adell, A., Artigas, F. (2004). The therapeutic role of 5-HT_{1A} and 5-HT_{2A} receptors in depression. *J Psychiatry Neurosci 29*: 252–265.

Chen, H.-S. V., Lipton, S. A. (2006). The chemical biology of clinically tolerated NMDA receptor antagonists. *J Neurochem* 97: 1611–1626.

Chu, D. C. M., Penney, J. B., Young, A. B. (1987). Cortical $GABA_B$ and $GABA_A$ receptors in Alzheimer's disease: A quantitative autoradiographic study. *Neurology 37*: 1454–1459.

Conde, F., Maire-Lepoivre, E., Audinat, E., Crepel, F. (1995a). Afferent connections of the medial frontal cortex of the rat. II. Cortical and subcortical afferents. *J Comp Neurol 352*: 567–593.

Conde, F., Maire-Lepoivre, E., Audinat, E., Crepel, F. Conde, F., Maire-Lepoivre, E., Audinat, E., Crepel, F. (1995b). Afferent connections of the medial frontal cortex of the rat. II. Cortical and subcortical afferents. *J Comp Neurol 352*: 567–593.

Coppen, A., Wood, K. (1982). Five-hydroxytryptamine in the pathogenesis of affective disorders. *Adv Biochem Psychopharmacol 34*: 249–258.

Cowan, R. L., Sesak, S. R., Van Bockstaele, E. J., Branchereau, P., Chain, J., Pickel, V. M. (1994). Analysis of synaptic inputs and targets of physiologically characterized neurons in rat frontal cortex: combined intracellular recording and immunolabelling. *Synapse 17*: 101–114.

Cull-Candy, S., Kelly, L., Farrant, M. (2006). Regulation of Ca2+-permeable AMPA receptors: synaptic plasticity and beyond. *Curr Opin Neurobio* 16: 288–297.

Danysz, W., Parsons, C. G., Möbius, H. J., Stoffler, A., Quack, G. (2000). Neuroprotective and symptomatological action of memantine relevant for Alzheimer's disease: a unified glutamatergic hypothesis on the mechanism of action. *Neurotox Res 2*: 85–97.

de Rover, M., Mansvelder, H. D., Lodder, J. C., Wardeh, G., Schoffelmeer, A. N., Brussaard, A. B. (2004). Long-lasting nicotinic modulation of GABAergic synaptic transmission in the rat nucleus accumbens associated with behavioural sensitization to amphetamine. *European Journal of Neuroscience 19*: 2859–2870.

Devoto, P., Flore, G., Pani, L., Gessa, G. L. (2001). Evidence for co-release of noradrenaline and dopamine from noradrenergic neurons in the cerebral cortex. *Molecular Psychiatry 6*: 657–664.

Drew, G. M., Vaughan, C. W. (2004). Multiple metabotropic receptor subtypes modulate GABAergic neurotransmission in rat periaqueductal grey neurons in vitro. *Neuropharmacology 46*: 927–934.

Ellison, Z., Foong, J., Howard, R., Bullmore, E., Williams, S., Treasure, J. (1998). Functional anatomy of calorie fear in anorexia nervosa. *Lancet 352*: 1192.

Franco, R., Ciruela, F., Casado, V., Cortes, A., Canela, E. I., Mallol, J, Agnati, L. F., Ferre, S., Fuxe, K., Lluis, C. (2005). Partners for adenosine A1 receptors. *J Mol Neurosci 26*: 221–232.

Frandsen, A., Schousboe, A. (2003). AMPA receptor-mediated neurotoxicity: Role of Ca^{2+} and desensitization. *Neurochem Res 28*: 1495–1499.

Frank, G. K., Bailer, U. F., Henry, S. E., Wagner, A., Kaye, W. H. (2004). Neuroimaging studies in eating disorders. *CNS Spectrums 9*: 539–548.

Gaddum, J. H., Hameed, K. A. (1954). Drugs which antagonize 5-hydroxytryptamine. *Br J Pharmacol Chemother 9*: 240–248.

Geyer, S., Matelli, M., Luppino, G., Schleicher, A., Jansen, Y., Palomero-Gallagher, N., Zilles, K. (1998). Receptor autoradiographic mapping of the mesial motor and premotor cortex of the macaque monkey. *J Comp Neurol 397*: 231–250.

Glenthøj, B. Y., Hemmingsen, R. (1999). Transmitter dysfunction during the process of schizophrenia. *Acta Psychiatr Scand 99*: 105–112.

Grønli, J., Fiske, E., Murison, R., Bjorvatn, B., Sorensen, E., Ursin, R., Portas, C. M. (2007). Extracellular levels of serotonin and GABA in the hippocampus after chronic mild stress in rats. A microdialysis study in an animal model of depression. *Behav Brain Res 181*: 42–51.

Hall, H., Lundkvist, C., Halldin, C., Farde, L., Pike, V. W., McCarron, J. A., Fletcher, A., Cliffe, I. A., Barf, T., Wikstrom, H., Sedvall, G. (1997). Autoradiographic localization of 5-HT1A receptors in the post-mortem human brain using [^{3}H]WAY-100635 and [^{11}C]way-100635. *Brain Res 745*: 96–108.

Hanson, E., Ronnback, L. (1992). Adrenergic receptor regulation of amino acid neurotransmitter uptake in astrocytes. *Brain Res Bull 29*: 297–301.

Heckers, S., Weiss, A. P., Deckersbach, T., Goff, D. C., Morecraft, R. J., Bush, G. (2004). Anterior cingulate cortex activation during cognitive interference in schizophrenia. *Am J Psychiatry 161*: 707–715.

Hendry, S. H., Huntsman, M.-M., Viñuela, A., Möhler, H., de Blas A. L., Jones, E. G. (1994). $GABA_A$ receptor subunit immunoreactivity in primate visual cortex: Distribution in macaques and humans and regulation by visual input in adulthood. *J Neurosci 14*: 2383–2401.

Hoyer, D., Hannon, J. P., Martin, G. R. (2002). Molecular, pharmacological and functional diversity of 5-HT receptors. *Pharmacol Biochem Behav 71*: 533–554.

Jansen, K. L., Faull, R. L. M., Dragunow, M. (1989). Excitatory amino acid receptors in the human cerebral cortex: a quantitative autoradiographic study comparing the distributions of TCP, [^{3}H]glycine, L-[^{3}H]-glutamate, [^{3}H]AMPA and [^{3}H]kainic acid binding sites. *Neuroscience 32*: 587–607.

Johnson, S. C., Schmitz, T. W., Moritz, C. H., Meyerand, M. E., Rowley, H. A., Alexander, A. L., Hansen, K. W., Gleason, C. E., Carlsson, C. M., Ries, M. L., Asthana, S., Chen, K., Reiman, E. M., Alexander, G. E. (2005). Activation of brain regions vulnerable to Alzheimer's disease: The effect of mild cognitive impairment. *Neurobiol Aging 27*: 1604–1612.

Kaye, W. H., Bailer, U. F., Frank, G. K., Wagner, A., Henry, S. E. (2005). Brain imaging of serotonin after recovery from anorexia and bulimia nervosa. *Physiology & Behavior 85*: 73–81.

Kjaer, T. W., Nowak, M., Lou, H. C. (2002). Reflective self-awareness and conscious states: PET evidence for a common midline parietofrontal core. *Neuroimage 17*: 1080–1086.

Kwak, S., Weiss, J. H. (2006). Calcium-permeable AMPA channels in neurodegenerative disease and ischemia. *Curr Opin Neurobio 16*: 281–287.

Lee, H.-K., Choi, S.-S., Han, K.-J., Han, E.-J., Suh, H.-W. (2004). Roles of adenosine receptors in the regulation of kainic acid induced neurotoxic responses in mice. *Mol Brain Res 125*: 76–85.

Lidov, H. G., Grzanna, R., Molliver, M. E. (1980). The serotonin innervation of the cerebral cortex in the rat - an immunohistochemical analysis. *Neuroscience 5*: 207–227.

Macdonald, R. L., Olsen, R. W., Macdonald, R. L., Olsen, R. W. (1994). $GABA_A$ receptor channels. *Annu Rev Neurosci 17*: 569–602.

Malizia, A. L., Cunningham, V. J., Bell, C. J., Liddle, P. F., Jones, T., Nutt, D. J. (1998). Decreased brain $GABA_A$-benzodiazepine receptor binding in panic disorder. *Arch Gen Psychiatry 55*: 715–720.

Marek, G. J., Aghajanian, G. K. (1999). 5-HT_{2A} receptor or α_1-adrenoceptor activation induces excitatory postsynaptic currents in layer V pyramidal cells of the medial prefrontal cortex. *Eur J Pharmacol 367*: 197–206.

Matsumoto, K., Puia, G., Dong, E., Pinna, G. (2007). GABA(A) receptor neurotransmission dysfunction in a mouse model of social isolation-induced stress: possible insights into a non-serotonergic mechanism of action of SSRIs in mood and anxiety disorders. *Stress 10*: 3–12.

Mayberg, H. S., Brannan, S. K., Mahurin, R. K., Jerabek, P. A., Brickman, J., Tekell, J. L., *et al.* (1997). Cingulate function in depression: a potential predictor of treatment response. *NeuroReport 8*: 1057–1061.

Meltzer, H. Y., Lowy, M. T. (1987). The serotonin hypothesis of depression. In: Psychopharmacology: the third generation of progress. H. Y. Meltzer, Ed. pp. 513–526. Raven Press, New York.

Milano, W., Petrella, C., Sabatino, C., Capasso, A. (2004). Treatment of bulimia nervosa with sertraline: a randomized controlled trial. *Adv Ther 21*: 232–237.

Molinuevo, J. L., Lladró, A., Rami, L. (2005). Memantine: Targeting glutamate excitotoxicity in ALzheimer's disease and other dementias. American Journal of Alzheimer's disease and Other *Dementias 20*: 77–85.

Morosan, P., Rademacher, J., Palomero-Gallagher, N., Zilles, K. (2004). Anatomical organization of the human auditory cortex: Cytoarchitecture and transmitter receptors. In: Auditory Cortex – Towards a Synthesis of Human and Animal Research. P. Heil,

E. König, E. Budinger, Eds. pp. 27–50. Lawrence Erlbaum, Mahwah, New Jersey.

Neumeister, A., Bain, E., Nugent, A. C., Carson, R. E., Bonne, O., Luckenbaugh, D. A., Eckelman, W., Herscovitch, P., Charney, D. S., Drevets, W. C. (2004). Reduced serotonin type 1_A receptor binding in panic disorder. *J Neurosci 24*: 589–591, 2004.

Northoff, G., Walter, M., Schulte, R. F., Beck, J., Dydak, U., Henning, A., Boeker, S., Grimm, S., Boesiger, P. (2007). GABA concentrations in the human anterior cingulate cortex predict negative BOLD responses in fMRI. *Nature Neuroscience 10*: 1515–1517.

Nutt, D. J., Malizia, A. L. (2001). New insights into the role of the $GABA_A$-benzodiazepine receptor in psychiatric disorder. *Br J Psychiatry 179*: 390–396.

Palomero-Gallagher, N., Vogt, B. A., Mayberg, H. S., Schleicher, A., Zilles, K. (2008). Receptor architecture of human cingulate cortex: Evaluation of the four region neurobiological model. *Human Brain Mapping*, in press.

Palomero-Gallagher, N., Mohlberg H., Zilles K., Vogt, B. A. (2008). Cytology and receptor architecture of human anterior cingulate cortex. *J. Comp. Neurol. 508*: 906–926.

Palomero-Gallagher, N., Zilles, K. (2004). The rat isocortex. In: The Rat Nervous System. F. Paxinos, Ed. pp. 729–757. Academic Press, San Diego.

Pasqualetti, M., Nardi, I., Ladinsky, H., Marazitti, D., Cassano, G. B. (1996). Comparative anatomical distribution of serotonin 1A, 1D? and 2A receptor mRNAs in human brain postmortem. *Mol Brain Res 39*: 223–233.

Pazos, A., Probst, A., Palacios, J. M. (1987a). Serotonin receptors in the human brain. III. Autoradiographic mapping of serotonin-1 receptors. *Neuroscience 21*: 97–122.

Pazos, A., Probst, A., Palacios, J. M. (1987b). Serotonin receptors in the human brain. IV. Autoradiographic mapping of serotonin-2 receptors. *Neuroscience 21*: 123–139.

Perry, D. C., Kellar, K. J. (1995). [^{3}H]Epibatidine labels nicotinic receptors in rat brain: an autoradiographic study. *J Pharmacol Exp Ther 275*: 1030–1034.

Porter, R. H. P., Eastwood, S. L., Harrison, P. J. (1997). Distribution of kainate receptor subunit mRNAs in human hippocampus, neocortex and cerebellum, and bilateral reduction of hippocampal GluR6 and KA2 transcripts in schizophrenia. *Brain Res 751*: 217–231, 1997.

Posner, M. I., Rothbart, M. K. (1998). Attention, self-regulation and consciousness. *Philos Trans R Soc London B Biol Sci 353*: 1915–1927.

Rakic, P., Goldman-Rakic, P. S., Gallager, D. W. (1988). Quantitative autoradiography of major neurotransmitter receptors in the monkey striate and extrastriate cortex. *J Neurosci 8*: 3670–3690.

Randrup, A., Munkvad, I. (1965). Special antagonism of amphetamine-induced abnormal behaviour. Inhibition of stereotyped activity with increase of some normal activities. *Psychopharmacologia 7*: 416–422.

Reynolds, G. P. (1995). Neurotransmitter systems in schizophrenia. *Int Rev Neurobiol 38*: 305–339.

Rodriguez-Puertas, R., Pascual, J., Vilaró, M. T., Pazos, A. (1997). Autoradiographic distribution of M1, M2, M3, and M4 muscarinic receptor subtypes in Alzheimer's disease. *Synapse* 26: 341–350.

Scheperjans, F., Grefkes, C., Palomero-Gallagher, N., Schleicher, A., Zilles, K. (2005). Subdivisions of human parietal area 5 revealed by quantitative receptor autoradiography: a parietal region between motor, somatosensory and cingulate cortical areas. *Neuroimage 25*: 975–992.

Schröder, H., Zilles, K., Maelicke, A., Hajos, F. (1989). Human cortical neurons contain both nicotinic and muscarinic acetylcholine receptors: an immunocytochemical double-labeling study. *Synapse 4*: 319–326.

Seamans, J. K., Yang, C. R. (2004). The principal features and mechanisms of dopamine modulation in the prefrontal cortex. *Progress in Neurobiology 74*: 1–57.

Seedat, S., Warwick, J., van Heerden, B., Hugo, C., Zungu-Dirwayi, N., van Kradenburg, J., Stein, D. J. (2004). Single photon emission computed tomography in posttraumatic stress disorder before and after treatment with a selective serotonin reuptake inhibitor. *J Affect Disord 80*: 45–53.

Seeman, P., Lee, T., Chau-Wong, M., Wong, K. (1976). Antipsychotic drug doses and neuroleptic/dopamine receptors. *Nature 261*: 717–719.

Sesack, S. R., Snyder, C. L., Lewis, D. A. (1995). Axon terminals immunolabeled for dopamine or tyrosine hydroxylase synapse on GABA-immunoreactive dendrites in rat and monkey cortex. *J Comp Neurol 363*: 264–280.

Smith, G. S., Ma, Y., Dhawan, V., Gunduz, H., Carbon, M., Kirshner, M., Larson, J., Chaly, T., Belakheff, A., Kramer, E., Greenwald, B., Kane, J. M., Laghrissi-Thode, F., Pollock, B. G., Eidelber, D. (2002). Serotonin modulation of cerebral glucose metabolism measured with positron emission tomography (PET) in human subjects. *Synapse 45*: 105–112.

Takano, A., Shiga, T., Kitagawa, N., Koyama, T., Katoh, C., Tsukamoto, E. (2001). Abnormal neuronal network in anorexia nervosa studied with I-123-IMP SPECT. *Psychiatry Research 107*: 45–50.

Thierry, A. M., Blanc, G., Sobel, A., Stinus, L., Glowinski, J. (1973). Dopaminergic terminals in the rat cortex. *Science 182*: 501.

Trudeau, L.-E. (2004). Glutamate co-transmission as an emerging concept in monoamine neuron function. *J Psychiatry Neurosci 29*: 296–310.

Uher, R., Brammer, M. J., Murphy, T., Campbell, I. C., Ng, V. W., Williams, S. C., Treasure, J. (2003). Recovery and chronicity in anorexia nervosa: brain activity associated with differential outcomes. *Biol Psychiatry 54*: 934–942.

Uher, R., Murphy, T., Brammer, M. J., Dalgleish, T., Phillips, M. L., Ng, V. W., Andrew, C. M., Williams, S. C., Campbell, I. C., Treasure, J. (2004). Medial prefrontal cortex activity associated with symptom provocation in eating disorders. *Am J Psychiatry 161*: 1238–1246.

Uher, R., Murphy, T., Friederich, H. C., Dalgleish, T., Brammer, M. J., Giampietro, V., Phillips, M. L., Andrew, C. M., Ng, V. W., Williams, S. C., Campbell, I. C., Treasure, J. (2005). Functional neuroanatomy of body shape perception in healthy and eating-disordered women. *Biol Psychiatry 58*: 990–997.

Vaiva, G., Boss, V., Ducrocq, F., Fontaine, M., Devos, P., Brunet, A., Laffargue, P., Goudemand, M., Thomas, P. (2006). Relationship between posttrauma GABA plasma levels and PTSD at 1-year follow-up. *Am J Psychiatry 163*: 1446–1448.

Vaiva, G., Thomas, P., Ducrocq, F., Fontaine, M., Boss, V., Devos, P., Rascle, C., Cottencin, O., Brunet, A., Laffargue, P., Goudemand, M. (2004). Low posttrauma GABA plasma levels as a predictive factor in the development of acute posttraumatic stress disorder. *Biol Psychiatry 55*: 250–254.

van der Zee, E. A., Luiten, P. G. M. (1999). Muscarinic acetylcholine receptors in the hippocampus, neocortex and amygdala: A review of immunocytochemical localization in relation to learning and memory. *Progress Neurobiol 58*: 409–471.

Versijpt, J., Van Laere, K. J., Dumont, F., Decoo, D., Vandecapelle, M., Santens, P., Goethals, I., Audenaert, K., Slegers, G., Dierckx, R. A. (2003). Imaging of the 5-HT_{2A} system: age-, gender-, and Alzheimer's disease-related findings. *Neurobiol Aging 24*: 553–561.

Vickers, J. C., Huntley, G. W., Hof, P. R., Bederson, J., DeFelipe, J., Morrison, J. H. (1995). Immunocytochemical localization of non-NMDA ionotropic excitatory amino acid receptor subunits in human neocortex. *Brain Res 671*: 175–180.

Vogt, B. A. (1993). Structural organization of cingulate cortex: areas, neurons, and somatodendritic transmitter receptors. In: Neurobiology of cingulate cortex and limbic thalamus. A comprehensive handbook. B. A. Vogt and M. Gabriel, Eds. pp. 19–70. Birkhäuser, Boston, Basel, Berlin.

Vogt, B. A., Berger, G. R., Derbyshire, S. W. G. (2003). Structural and functional dichotomy of human midcingulate cortex. *Eur J Neurosci 18*: 3134–3144.

Vogt, B. A., Crino, P. B., Vogt, L. (1992). Reorganization of cingulate cortex in Alzheimer's disease: neuron loss, neuritic plaques, and muscarinic receptor binding. *Cerebral Cortex 2*: 526–535.

Vogt, B. A., Crino, P. B., Volicer, L. (1991). Laminar alterations in γ-aminobutyric $acid_A$, muscarinic, and β adrenoceptors and neuron degeneration in cingulate cortex in Alzheimer's disease. *J Neurochem 57*: 282–290.

Vogt, B. A., Nimchinsky, E. A., Vogt, L., Hof, P. R. (1995). Human cingulate cortex: surface features, flat maps, and cytoarchitecture. *J Comp Neurol 359*: 490–506.

Vogt, B. A., Sikes, R. W., Vogt, L. J. (1990). Anterior cingulate cortex and the medial pain system. In: The Cerebral Cortex of the Rat. B. Kolb and R. C. Tees, Eds. pp. 313–344, 1990. MIT, Cambridge, MA.

Vogt, B. A., Vogt, L. (2003). Cytology of human dorsal midcingulate and supplementary motor cortices. *J Chem Neuroanat 26*: 301–309.

Vogt, B. A., Vogt, L., Perl, D. P., Hof, P. R. (2001). Cytology of human caudomedial cingulate, retrosplenial, and caudal parahippocampal cortices. *J Comp Neurol 438*: 376.

Volkow, N. D., Fowler, J. S., Wang, G. J., Swanson, J. M. (2004). Dopamine in drug abuse and addiction: results from imaging studies and treatment implications. *Mol Psychiatry 9*: 557–569.

Wadenberg, M.-L., Salmi, P., Jimenez, P., Svensson, T., Ahlenius, S. (1996). Enhancement of antipsychotic-like properties of the dopamine D_2 receptor antagonist, raclopride, by additional treatment with the 5-HT2 receptor blocking agent, ritanserin, in the rat. *Eur Neuropsychopharmacol 305*.

Wenk, G. L. (2006). Neuropathologic changes in Alzheimer's disease: Potential targets for treatment. *J Clin Psychiatry 67*: 3–7.

Wenk, G. L., Barnes, C. A. (2000). Regional changes in the hippocampal density of AMPA and NMDA receptors across the lifespan of the rat. *Brain Res 885*: 1–5.

West, A. R., Floresco, S. B., Charara, A., Rosenkranz, J. A., Grace, A. A. (2003). Electrophysiological interactions between striatal glutamatergic and dopaminergic systems. *Ann NY Acad Sci 1003*: 53–74.

Wolf, M. E., Mangiavacchi, S., Sun, X. (2003). Mechanisms by which dopamine receptors may influence synaptic plasticity. *Ann NY Acad Sci 1003*: 241–249.

Woolley, D. W., Shaw E. (1954). A biochemical and pharmacological suggestion about certain mental disorders. *Proc Natl Acad Sci* USA *40*: 228–231, 1954.

Zilles, K., Eickhoff, S., Palomero-Gallagher, N. (2003). The human parietal cortex: a novel approach to its architectonic mapping. *Adv Neurol 93*: 1–21.

Zilles, K., Palomero-Gallagher, N. (2001). Cyto-, myelo-, and receptor architectonics of the human parietal cortex. *Neuroimage 14*: S8-S20.

Zilles, K., Palomero-Gallagher, N., Grefkes, C, Scheperjans, F., Boy, C., Amunts, K., Schleicher, A. (2002a). Architectonics of the human cerebral cortex and transmitter receptor fingerprints: reconciling functional neuroanatomy and neurochemistry. *European Neuropsychopharmacology 12*: 587–599.

Zilles, K., Palomero-Gallagher, N., Schleicher, A. (2004). Transmitter receptors and functional anatomy of the cerebral cortex. *J Anat 205*: 417–432.

Zilles, K., Schlaug, G., Matelli, M., Luppino, G., Schleicher, A., Qü, M., Dabringhaus, A., Seitz, R., Roland, P. E. (1995). Mapping of human and macaque sensorimotor areas by integrating architectonic, transmitter receptor, MRI and PET data. *J Anat 187*: 515–537.

Zilles, K., Schleicher, A., Palomero-Gallagher, N., Amunts, K. (2002b). Quantitative analysis of cyto- and receptorarchitecture of the human brain. In: Brain Mapping. The Methods. A. W. Toga and J. C. Mazziotta, Eds. pp. 573–602. Elsevier, Amsterdam.